

Review

Solar Window Innovations: Enhancing Building Performance through Advanced Technologies

Mehrdad Ghamari  and Senthilarasu Sundaram * 

School of Computing, Engineering and Digital Technologies, Teesside University, Tees Valley, Middlesbrough TS1 3BX, UK; mehrdad.ghamari.9.7@gmail.com

* Correspondence: s.sundaram@tees.ac.uk

Abstract: Building-integrated photovoltaic (BIPV) glazing systems with intelligent window technologies enhance building energy efficiency by generating electricity and managing daylighting. This study explores advanced BIPV glazing, focusing on building-integrated concentrating photovoltaic (BICPV) systems. BICPV integrates concentrating optics, such as holographic films, luminescent solar concentrators (LSC), Fresnel lenses, and compound parabolic concentrators (CPCs), with photovoltaic cells. Notable results include achieving 17.9% electrical efficiency using cylindrical holographic optical elements and crystalline silicon cells at a $3.5\times$ concentration ratio. Dielectric CPCs showed 97.7% angular acceptance efficiency in simulations and 94.4% experimentally, increasing short-circuit current and maximum power by 87.0% and 96.6%, respectively, across 0° to 85° incidence angles. Thermochromic hydrogels and thermotropic smart glazing systems demonstrated significant HVAC energy savings. Large-area 1 m^2 PNIPAM-based thermotropic window outperformed conventional double glazing in Singapore. The thermotropic parallel slat transparent insulation material (TT PS-TIM) improved energy efficiency by up to 21.5% compared to double glazing in climates like London and Rome. Emerging dynamic glazing technologies combine BIPV with smart functions, balancing transparency and efficiency. Photothermally controlled methylammonium lead iodide PV windows achieved 68% visible light transmission, 11.3% power conversion efficiency, and quick switching in under 3 min. Polymer-dispersed liquid crystal smart windows provided 41–68% visible transmission with self-powered operation.

Keywords: solar windows; building-integrated photovoltaics (BIPVs); zero-energy buildings; energy efficiency; concentrating optics; thermotropic smart glazing; dynamic glazing technologies



Citation: Ghamari, M.; Sundaram, S. Solar Window Innovations: Enhancing Building Performance through Advanced Technologies. *Energies* **2024**, *17*, 3369. <https://doi.org/10.3390/en17143369>

Academic Editor: Philippe Leclère

Received: 13 June 2024

Revised: 6 July 2024

Accepted: 8 July 2024

Published: 9 July 2024



Copyright: © 2024 by the authors. Licensee MDPI, Basel, Switzerland. This article is an open access article distributed under the terms and conditions of the Creative Commons Attribution (CC BY) license (<https://creativecommons.org/licenses/by/4.0/>).

1. Introduction

In a period characterized by growing worldwide apprehension regarding climate change and environmental conservation, it is imperative to prioritize the tackling of energy inefficiency and the emission of greenhouse gases (GHG). The construction and building industries have taken center stage in this endeavor due to their substantial consumption of resources and energy, which exerts immense pressure on natural ecosystems and limited resources [1–3].

The scale of this challenge is staggering. The International Energy Agency (IEA) indicates that over 30% of worldwide energy is utilized in buildings [4]. This significant energy consumption is not only a drain on resources but also a major contributor to global carbon emissions. The building sector's impact on climate change is further exacerbated by inefficient design and outdated technologies, particularly in older structures that lack modern energy-saving features.

One of the most critical areas of concern is the management of solar radiation in buildings. Especially in summertime, solar radiation penetrating rooms via windows can notably elevate the energy usage of air-conditioning systems, especially in newly built high-rise structures with extensive window-to-wall ratios [5]. This phenomenon is particularly

problematic in urban areas where the proliferation of glass-facade skyscrapers has led to increased cooling demands and, consequently, higher energy consumption.

Thus, diminishing solar radiation infiltration through windows presents an effective strategy for curbing cooling demands and energy usage in air conditioning [6]. This approach not only reduces energy consumption but also improves indoor comfort levels and can lead to significant cost savings for building operators and occupants. Innovative window technologies, such as smart glass and advanced shading systems, are being developed and implemented to address this issue.

The worldwide attention to combatting climate change and promoting environmental sustainability has resulted in the setting of ambitious goals for energy-efficient building practices. These goals reflect a growing recognition of the urgent need to transform the building sector to meet climate targets and ensure a sustainable future. In the United States, there was an expectation for all new commercial building projects to attain zero-energy status by 2030 [7]. This ambitious target has spurred innovation in building design, materials, and technologies, pushing the industry towards more sustainable practices.

Similarly, the European Union (EU) has proposed transitioning from the existing Nearly Zero-Energy Building (NZEB) standard to Zero-Emission Buildings (ZEBs), ensuring that energy performance requirements for new buildings are in line with the EU's broader climate neutrality goals [8]. This shift represents a significant step forward, moving beyond energy efficiency to address the total environmental impact of buildings throughout their lifecycle.

These initiatives are part of a broader global movement towards sustainable architecture and urban planning. Countries around the world are implementing stricter building codes, offering incentives for green construction, and investing in research and development of new sustainable building technologies. The focus is not just on new construction but also on retrofitting existing buildings to improve their energy performance.

The challenge of creating energy-efficient buildings goes beyond just reducing energy consumption. It also involves consideration of material sustainability, waste reduction, water conservation, and the overall impact of buildings on human health and well-being. This holistic approach to sustainable building design is driving innovations in areas such as biophilic design, which incorporates natural elements into buildings to improve air quality and occupant well-being.

A crucial element in meeting ambitious energy-efficiency goals involves adopting advanced building envelopes, which encompass insulation, windows, roofing, solar chimneys, and exterior walls [9,10]. These components are instrumental in regulating energy flow within structures, highlighting the critical importance of enhancing their performance to effectively reduce overall primary energy consumption in buildings. The building envelope serves as a barrier between indoor and outdoor environments, playing a vital role in maintaining thermal comfort and minimizing energy usage. Studies have shown that passive architectural strategies, including solar chimneys and Trombe walls, can improve thermal comfort by up to 20% and reduce electricity consumption by as much as 46% [9]. Furthermore, building-integrated photovoltaic (BIPV) systems, when applied to rooftops, windows, and facades, offer significant potential for energy generation and savings. However, challenges persist in the widespread adoption of these technologies, including economic feasibility, technical performance, and architectural considerations [10]. The integration of smart control systems for heating, ventilation, and air conditioning (HVAC) has demonstrated energy savings of 10–28%, while advanced lighting control can achieve savings of 43–71% [11]. These findings underscore the importance of a holistic approach to building design, incorporating not only envelope improvements but also occupant behavior and advanced technologies to achieve optimal energy efficiency [12].

Among these components, windows have emerged as a critical focus area due to their significant impact on both energy performance and occupant comfort. Traditional windows, while providing natural light and views, can be a major source of heat gain in summer and heat loss in winter, contributing to increased energy demands for cooling and heating.

The influence of windows on building energy consumption is a complex issue. Traditional windows with a high solar heat gain coefficient (SHGC) and visible light transmittance (τ_{vis}) can lead to excessive heat and glare, necessitating solar shading solutions [13]. However, these shading devices may block useful daylight, increasing reliance on artificial lighting and energy consumption. Smart windows offer a dynamic solution to this challenge. For instance, polymer-dispersed liquid crystal (PDLC) glazing can switch between translucent and transparent states, providing low ultraviolet (UV) (8%) and near infrared (NIR) (44%) transmission in its translucent state, with SHGC values of 0.68 and 0.63 for transparent and translucent states, respectively [13]. Electrochromic windows controlled by operative temperature have shown the highest potential for reducing energy demand across various climates [14]. In tropical regions, semi-transparent photovoltaic (STPV) glazing can offer both solar control and on-site electricity generation, with SHGC reducing significantly at incident angles above 45° [15]. For subtropical climates, an optimum overhang and fin height equal to half the window height can lead to significant energy savings, with one study reporting a 7.05% reduction in annual energy consumption [16]. These advances create a complex balancing act between managing solar heat gain, maintaining adequate natural light, and minimizing energy use while potentially generating electricity.

The energy efficiency of buildings is influenced by multiple factors, including lighting performance, electrical generation, and thermal properties [17,18]. Window performance is evaluated through various metrics, each addressing specific aspects of energy efficiency. Electrical performance is typically assessed based on photovoltaic (PV) conversion efficiency and electricity generation per square meter, particularly relevant for BIPV components. Thermal performance is mainly evaluated using metrics such as SHGC and U-value (heat transfer coefficient) [19]. Studies have shown that advanced window technologies can significantly impact energy consumption. For instance, switchable windows can reduce annual heating and cooling energy by up to 59.1% and 64.9%, respectively, in certain U.S. climates [19]. BIPV components with optimized design parameters can also offer substantial benefits. Geometric transparency degree (GTD) has been found to most significantly affect optical properties, with SHGC and visible transmittance (VT) positively correlating with GTD [20].

In response to these challenges, innovative solar window technologies have been developed to transform windows from passive elements into active energy-generating components of the building envelope. Integrating PV cells into windows or shading devices, known as BIPV, presents a promising solution to these challenges [21]. BIPV windows can replace conventional windows entirely, generating electricity while reducing solar radiation entering the building, thus decreasing the power consumption of air-conditioning systems [22].

BIPV windows come in various forms, each with unique characteristics and applications [21,22]:

Crystalline Silicon Solar Cells: These are the most common type of PV cells used in BIPV windows. They offer high efficiency but can be opaque, making them suitable for spandrel areas or where transparency is not required.

Thin-Film Solar Cells: These cells can be made semi-transparent and are more flexible in application. While they typically have lower efficiency than crystalline silicon, they perform better in low-light conditions and at high temperatures.

Dye-Sensitized Solar Cells (DSSCs): These cells can be made in various colors and transparencies, offering aesthetic versatility. They are particularly effective in low-light conditions and can be integrated into windows without significantly compromising visibility.

Perovskite Solar Cells: A newer technology that has shown rapid improvements in efficiency. Perovskite cells can be made semi-transparent and have the potential to offer high efficiency at a lower cost than traditional silicon cells.

Quantum Dot Solar Windows: These utilize quantum dots to absorb sunlight and re-emit it at infrared wavelengths that can be captured by PV cells at the edges of the window. This technology allows for highly transparent solar windows.

Beyond electricity generation, solar windows can also contribute to passive solar design strategies. Passive solar systems, like solar walls (SWs), are significant developments in enhancing the thermal storage ability of materials and improving heat transfer processes [23]. SWs, also known as Trombe walls, consist of a dark-colored wall with a glass exterior and an air space in between. They work by absorbing solar radiation during the day, storing it as heat in the wall's thermal mass, and then releasing it into the building at night or during cooler periods. This passive solar heating can significantly reduce the need for active heating systems, particularly in colder climates [24]. The integration of passive solar systems such as SWs into building envelopes, coupled with advancements in energy storage materials, has the potential to boost solar energy as a sustainable alternative, thus raising energy efficiency standards [25,26].

The main objective of this research is to assess the notable impact of merging photovoltaics with thermal regulation, particularly through SW, in addressing challenges within the construction and building sector. This study will conduct an in-depth examination of relevant literature, concentrating on the operational principles of SW and past research in this field.

This investigation aims to elucidate how innovative building envelope solutions can play a crucial role in establishing a sustainable and energy-efficient built environment, making significant contributions to global efforts in combating climate change and alleviating the negative impacts of environmental deterioration [27]. The building sector accounts for over one-third of global energy consumption and a significant share of carbon emissions, emphasizing the urgent need for improved energy efficiency, particularly in tropical regions where future development is concentrated. Building-integrated photovoltaic thermal (BIPV/T) systems within building façades can successfully produce both electrical and thermal energy, thus improving buildings' energy performance. These systems can overcome space constraints in urban areas by utilizing building façades for energy production, potentially reducing up to 40% of global energy demand [28].

Comprehensive reviews of building envelope design variables in tropical climates have shown that insulation, glazing properties, and window-to-wall ratio (WWR) are promising solutions for improving energy efficiency. Optimized designs in cooling-dominated climates can save 35% of annual energy and up to 60% in some cases [29].

Phase change material (PCM) solar walls, as a low-carbon technology, have shown potential in both cold and warm seasons. Experimental investigations revealed that PCM solar walls could maintain comfortable indoor temperatures for extended periods—up to 7 h above 20 °C during the heating season and within the comfort range for about 17 h during the cooling season. By capturing solar radiation during the day and releasing stored energy at night, these systems optimize energy utilization, lessening reliance on conventional energy sources and resulting in substantial energy and carbon footprint reductions [30].

This research provides an innovative and comprehensive exploration of integrating photovoltaics with thermal regulation in sustainable building design, specifically focusing on SW. The study uniquely synthesizes various cutting-edge technologies, including crystalline, thin-film, and emerging PV cells, with advanced thermal management strategies.

The work's originality lies in its holistic approach, combining BICPV glazing systems with thermotropic smart glazing technologies. This integration addresses both energy generation and thermal regulation challenges in buildings, offering a novel solution to reduce energy waste and greenhouse gas emissions.

The research breaks new ground by analyzing the potential of various concentrating optics, such as diffused reflectors, holographic films, and luminescent solar concentrators (LSCs), in the context of building-integrated applications. It also explores innovative non-planar optics, like Fresnel lenses, prismatic lenses, and compound parabolic concentrators, for enhanced energy capture and daylighting control.

Furthermore, the study advances the field by examining the synergy between PV and electrochromic technologies in smart windows. This integration represents a forward-looking approach to creating energy-efficient and environmentally friendly buildings.

By comprehensively evaluating these diverse technologies and their potential combinations, this research contributes significantly to the development of next-generation sustainable building solutions. It provides valuable insights into optimizing energy performance, thermal comfort, and architectural aesthetics, paving the way for more efficient and visually appealing building exteriors that actively contribute to energy production and management.

2. Enhancing Building Energy Efficiency through Envelope Design

Enhancing building energy efficiency can be achieved through active or passive strategies. Active strategies involve improvements to systems, like HVAC and lighting, while passive strategies focus on optimizing building envelope components. There has been a renewed interest in environmentally friendly passive building energy efficiency strategies due to their effectiveness in addressing energy crises and environmental issues [31].

The building envelope plays a critical role in determining a building's energy efficiency by separating indoor and outdoor environments, controlling indoor conditions, and managing energy transfer between them [26,32,33]. Elements like walls, windows, roofs, foundations, insulation, thermal mass, and shading devices significantly impact the overall performance of the building envelope.

Numerous academic studies have highlighted the substantial influence of building envelope enhancements on energy usage. For instance, in the hot and humid climate of Hong Kong, the adoption of passive energy-efficient strategies, such as thermal insulation, reflective coatings, and shading devices, led to energy savings of 31.4% and peak load savings of 36.8% [34]. Similarly, in Greece, the utilization of thermal insulation, low infiltration strategies, and external shading resulted in energy consumption reductions of up to 40% [35].

The incorporation of PV cells into windows or shading mechanisms, referred to as building-integrated photovoltaics (BIPVs), presents a promising strategy for addressing energy efficiency issues in architectural structures [36]. BIPV windows have the potential to supplant conventional windows, generating electricity while mitigating solar heat gain, thereby reducing the energy consumption of air conditioning systems [5,37].

This investigation endeavors to assess the notable influence of integrating photovoltaics with thermal management, with a specific focus on solar window setups. By examining practical implementations and recent progressions in solar window technology, the objective is to unveil the pivotal role these innovative approaches can play in fostering sustainable and energy-efficient constructed environments. The primary aim of this research is to offer a substantive contribution to global endeavors aimed at combating climate change and advancing environmental sustainability.

The pursuit of energy efficiency in construction is a vital imperative, considering the prevailing global environmental dilemmas. Solar window systems emerge as a propitious pathway since they seamlessly incorporate PV and thermal regulation functionalities into building frameworks. This amalgamation holds the potential to revolutionize our methodologies for designing and erecting energy-efficient construction, paving the way towards a more sustainable and eco-friendly trajectory.

3. The Challenges Posed by Traditional Windows (e.g., Heat Gain, Glare, Energy Consumption)

Conventional windows present significant challenges in terms of heat transfer, glare, and energy use, all of which can significantly affect a building's overall energy performance. According to statistical evidence, windows can contribute to as much as 40% of heat dissipation in winter and up to 87% of heat accumulation in summer [38]. Overcoming these challenges is crucial for fostering sustainable building designs and reducing overall energy usage.

One major challenge with conventional windows is the excessive accumulation of heat. These windows are susceptible to heat transfer through conduction, convection, and radiation, leading to heightened cooling demands during warmer months [39]. This increased heat gain in warm climates can elevate energy consumption for air conditioning systems [40].

Figure 1 illustrates the factors influencing the performance and characteristics of windows. It presents two main mechanisms: heat conduction and solar heat gain. Heat conduction pertains to the transfer of heat across window materials such as glass, frames, air seals, and spacers between panels. This process is measured by the U_w value (thermal conductivity of the window), which represents its thermal conductivity. A lower U_w value indicates higher resistance to heat flow, indicating better insulation properties.

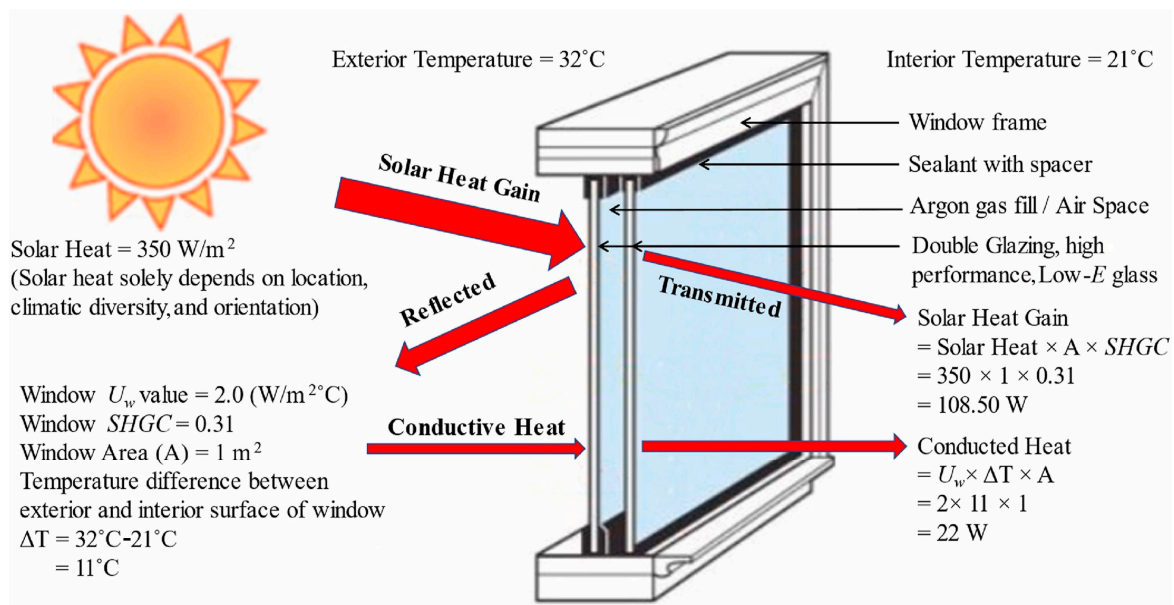


Figure 1. Schematic illustration of heat transfer mechanisms in an energy-efficient window [38].

Conversely, solar heat gain denotes the solar radiation infiltration through windows, leading to internal heat buildup. This parameter is quantified by the SHGC, which varies from 0 to 1. A lower SHGC implies that the window allows less incident solar heat radiation to pass through, thereby diminishing the heat transmitted, absorbed, and emitted within the building, consequently reducing heat gain through windows.

Figure 2 visually represents how these two mechanisms, heat conduction and solar heat gain, interact to influence the thermal performance of windows. It stresses the significance of taking into account both the U_w value and SHGC when creating energy-efficient windows for buildings. These factors are critical in managing heat transfer and solar heat gain, which in turn affect energy usage for heating and cooling needs [38].

Additionally, direct sunlight penetrating through windows can create glare, diminishing visual comfort and productivity and potentially escalating the use of artificial lighting, thereby adding to energy consumption [41].

Another significant challenge stems from the limited insulating properties of traditional windows, resulting in considerable heat loss during winter. This heat loss drives up the energy needed for space heating, contributing to higher overall energy consumption [42]. Integrating PV technology into windows provides additional benefits such as shading and glare control. Strategically positioning PV cells can block direct sunlight, lessening the need for external shading devices and enhancing visual comfort [43].

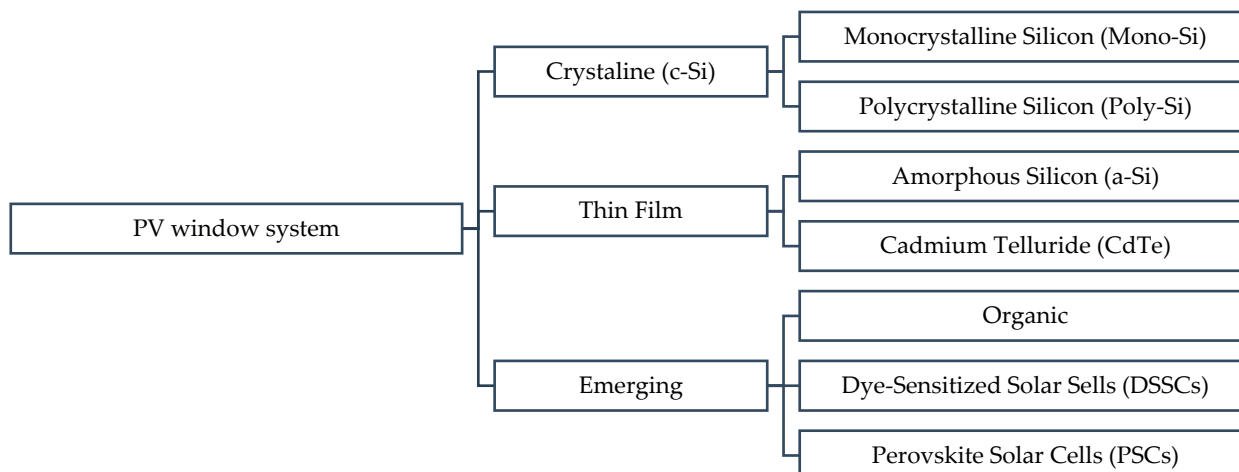


Figure 2. Classification of PV window system [21].

Another promising technology is the utilization of thermotropic materials for energy-efficient windows. Thermotropic materials are substances that change their properties in response to temperature variations. These materials typically undergo phase transitions or structural changes when exposed to different temperatures, altering their optical, mechanical, or electrical characteristics [44]. These materials possess the capability to reversibly modulate their light transmission properties, delivering holistic performance in terms of indoor thermal conditions, energy efficiency, and daylight utilization. Thermotropic double-glazed windows notably improved indoor thermal comfort in west-facing rooms when compared to conventional options. They lowered the cooling electricity needs by 19% in west-facing rooms while providing suitable indoor illumination [45].

Moreover, studies show that the energy efficiency of windows is affected not only by their thermal characteristics but also by climatic variations and the orientation of buildings. The angle at which solar radiation strikes the window surface has a substantial impact on heat transfer, with the highest transfer occurring when the sun is directly perpendicular to the glass surface [46].

4. Categorization of PV Window System

The PV window system encompasses a diverse range of technologies classified into three main categories: crystalline, thin film, and emerging solar cells. Each category represents distinct materials and manufacturing processes that influence their efficiency and suitability for BIPV applications. Figure 2 provides a visual representation of this categorization.

4.1. Crystalline PV Technologies

Monocrystalline Silicon (Mono-Si): These cells are created by slicing single-crystal silicon rods into thin wafers. Mono-Si cells are renowned for their high purity and effectiveness, achieving a peak cell efficiency of 26.1% for monocrystalline silicon, making it one of the most efficient PV technologies currently accessible [47,48].

Polycrystalline Silicon (Poly-Si): The manufacturing process includes melting silicon, shaping it into square ingots, and subsequently solidifying it into crystals with different orientations. This process results in lower purity compared to *Mono-Si* but is more cost-effective. The efficiency of poly-Si modules is enhanced through improved thermal regulation and ventilation strategies, especially in building-integrated applications [49,50].

4.2. Thin Film PV Technologies

Amorphous Silicon (a-Si): This thin-film technology is formed by applying thin layers of silicon onto a glass substrate using plasma-enhanced chemical vapor deposition. Despite having lower efficiency compared to crystalline silicon, typically around 9–14%, a-Si offers ad-

vantages such as flexibility and lower production costs. Its application in naturally ventilated PV-DSF and STPV glazings showcases its potential in various BIPV scenarios [51–54].

Cadmium Telluride (CdTe): The CdTe thin-film technology involves layers of CdTe deposited onto substrates. It is notable for its lower production costs compared to crystalline silicon. The effectiveness of CdTe modules in PV-DSF and STPV window glazings is demonstrated by superior performance ratios compared to traditional crystalline technologies in certain applications [55,56].

4.3. Emerging PV Technologies

Organic Solar Cells: These thin-film cells utilize organic materials as their active layer, providing benefits such as flexibility and the potential for cost-effective production. However, their efficiency tends to be lower, typically ranging from 3% to 12.6%. Their performance in BIPV arrays and energy-saving capabilities in glazings are notable, although challenges such as degradation over time and lower efficiency compared to inorganic counterparts persist [47,57,58].

Dye-Sensitized Solar Cells (DSSCs): The low cost, flexibility, and semi-transparency of DSSCs make them suitable for building applications. Their efficiency ranges from 7% to around 11.9%, depending on the specific design and materials used. Their potential is seen in various orientations, energy-saving applications, and glare-reduction strategies in building-integrated contexts [59].

Perovskite Solar Cells (PSCs): Attention has been gained by PSCs due to their rapidly improving efficiency, reaching up to 23.3% in research settings. They are relatively easy to manufacture and offer cost advantages compared to some traditional PV technologies. Their potential in energy-saving applications like PV-DSF is highlighted, showcasing their higher energy yield compared to other thin-film technologies, like DSSCs, under certain conditions [60].

Different PV panels exhibit varying response ranges to solar spectra, which significantly impacts their efficiency and performance. Recent research has explored innovative approaches to optimizing PV systems by incorporating spectral beam splitters (SBSs) using nanofluids. Hybrid nanofluids containing antimony tin oxide (ATO) and cupric oxide (CuO) nanoparticles can effectively regulate spectral absorption. ATO shows high absorption in the infrared region, while CuO strongly absorbs ultraviolet and visible light, allowing for complementary optical properties. By adjusting the nanoparticle composition and concentration, the spectral absorption can be fine-tuned across the full spectrum [61]. Another study investigated carbon quantum dot (CQD) nanofluids as SBSs in PV/thermal systems. These CQD-nanofluid filters exhibited ultra-stability and tunable optical properties, which could be adjusted by varying heating time and polyethylene glycol (PEG) concentration. This approach allowed for enhanced absorption across the whole spectrum and the regulation of absorption at specific wavelengths [62]. Table 1 presents a summary of important discoveries from multiple studies that examine the effects of PV window systems.

Table 1. PV window systems.

Ref.	Focus	Type	Key Findings
[63]	STPV	c-Si/a-Si	<ul style="list-style-type: none"> The EnergyPlus software (version 9.6), which is extensively used for building energy analysis, faced difficulties in modeling various STPV module types and failed to anticipate surface temperature rises during power generation. This underscores the necessity of improving simulation algorithms to precisely evaluate the energy efficiency of STPV systems in building contexts. Actual indoor temperatures (in Celsius) compared with simulation results: <ul style="list-style-type: none"> ✓ January (Winter): c-Si module—Mock-up: 7.2, Simulation: 6.0 a-Si module—Mock-up: 5.9, Simulation: 6.6 ✓ April (Spring): c-Si module—Mock-up: 18.4, Simulation: 14.7 a-Si module—Mock-up: 17.5, Simulation: 15.4 Maximum temperatures (in Celsius) based on mock-up vs. simulation: <ul style="list-style-type: none"> ✓ c-Si module: Mock-up—43.2, Simulation—20.01 ✓ a-Si module: Mock-up—44.4, Simulation—22.36

Table 1. Cont.

Ref.	Focus	Type	Key Findings
[64]	BIPV double-skin façade (DSF)	a-Si	<ul style="list-style-type: none"> The BIPV-DSF configuration is observed to notably decrease peak daylight illuminance by 73% compared to standard DSF. The mean and minimum daylight factors (0.65% and 0.00%, respectively) are found to fall short of the established visual comfort criteria indoors, particularly in office environments. BIPV-DSF is seen to increase building energy consumption by 8% over regular DSF in the UK's climate, making it non-viable for commercial installation.
[65]	CdTe Thin-Film Solar Cell Optimization	CdTe	<ul style="list-style-type: none"> A thin-film solar cell made of CdTe demonstrates a short-circuit current density of 29.09 mA/cm², an open-circuit voltage of 0.95 V, a fill factor of 83.47%, and achieves an efficiency of approximately 23% under AM1.5G irradiance.
[66]	Optimizing Window Layers	CdTe	<ul style="list-style-type: none"> Oxygenated cadmium sulfide (CdS:O) with a low series resistance ($R_s \leq 1 \text{ E}^{-1} \Omega\text{-cm}^2$) and a carrier concentration of 10^{16} cm^{-3} effectively aligns bands, enhancing photo-current collection across different wavelengths compared to standard CdS/CdTe cells. Addition of cadmium zinc sulfide (CdZnS) improves performance metrics (QE, J_{sc}, V_{oc}, η, FF), but carrier recombination and saturation current density are increased, leading to unstable performance. The incorporation of CdS:O improves conversion efficiency with J_{sc} (29.10 mA·cm⁻²), V_{oc} (0.889 V), and FF (70.39%), indicating its promise as a viable window material for CdTe thin-film solar cells in BIPV settings.
[67]	Transparent photovoltaics	Organic	<ul style="list-style-type: none"> The study revealed a positive net energy gain, with advantageous energy return on investment ranging from 102 in Phoenix for window applications to 208 in Honolulu for skylight applications. Energy payback times ranged from 51 days to 1.1 years, varying based on location and module type.
[68]	Flexible Solar Cells	Organic	<ul style="list-style-type: none"> Power conversion efficiencies (PCEs) exceeded 18%, while flexible OSCs (F-OSCs) reached over 15%, showcasing significant progress. Potential applications like IoT and electric vehicles are highlighted by F-OSCs, with solar modules being produced around 1.54 kWh/day in Beijing, aiding in reducing range anxiety in electric vehicles.
[60]	DSSC Windows for Energy Efficiency	DSSC	<ul style="list-style-type: none"> Enhanced heat transmission (U-value) and decreased visible-light transmission (VLT) compared to low-emissivity glazing result in reduced heating energy while increasing cooling and lighting energy. Significant annual energy savings of 4861.44 kWh are predicted, with DSSC windows meeting 13% PCE and 30% VLT criteria, highlighting their potential in energy-efficient building design.
[69]	Glazing Performance Analysis	DSSC	<ul style="list-style-type: none"> Power generation efficiency of DSSCs varies with incident solar energy, showcasing temporary increases. Performance order: red > green > blue; green at 56% and blue at 43% compared to red. Lower VLT leads to higher efficiency, with VLT 7% showing 157% and VLT 10% showing 133% performance over VLT 20%.
[70]	Enhancing Efficiency of Perovskite Solar Cells	PSCs	<ul style="list-style-type: none"> PSCs utilizing lead-based light harvesters achieve a power conversion efficiency of 25.5%. On the other hand, CsPbI₂Br perovskites exhibit enhanced thermal stability and carrier transport characteristics, achieving efficiencies ranging from 17.71% to 17.54% with different hole transport layers.
[71]	Perovskite Solar Cell Efficiency	PSCs	<ul style="list-style-type: none"> The antisolvent chlorobenzene (CB) is widely employed in the production of high-efficiency PSCs. A systematic exploration of CB antisolvent additives has yielded notable power conversion efficiencies of 22.22% and 19.74% for rigid and flexible devices, respectively.

5. Building-Integrated Concentrating PV Glazing

Building-integrated concentrating photovoltaic (BICPV) glazing combines the advantages of concentrating photovoltaics (CPVs) and BIPV to enhance electricity generation, daylight control, and aesthetics in buildings. These systems utilize concentrating optics to focus solar radiation onto PV cells integrated into windows or facades.

Figure 3 provides a comprehensive classification of BIPV concentrating optics, crucial components of BICPV systems categorized based on their geometric shapes. The categorization comprises flat plate optical elements (also known as planar) and non-planar optical elements. This specific focus enhances the efficiency of electricity generation while preserving natural daylighting and visual transparency.

BICPV glazing represents an innovative solution for sustainable building design, offering a balance between energy production and architectural integration, paving the way for more efficient and visually appealing building exteriors [72,73]. Planar concentrating

optics like diffused reflectors, holographic films, and LSCs, alongside non-planar options such as Fresnel lenses, wedge prisms, and compound parabolic concentrators (CPCs), offer diverse solutions for optimizing energy performance and architectural aesthetics in BICPV applications [74].

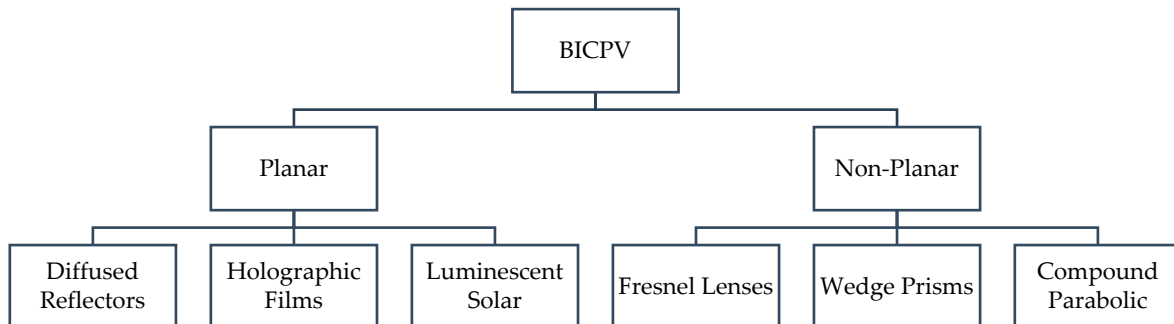


Figure 3. Classification of BIPV [74].

5.1. Planar Concentrating Optics

Flat-plate static solar concentrators (FPSCs) show great promise for BIPV applications. These concentrators can effectively capture and focus sunlight without requiring sun-tracking systems, making them well-suited for integration into buildings. Figure 4 illustrates different configurations of FPSCs used in solar energy systems. In Figure 4a, a sectional view shows FPSC modules that include v-grooved reflectors along with monofacial solar cells. Figure 4b showcases a similar setup but with bifacial solar cells. Both designs demonstrate how reflectors are placed between adjacent solar cells on a transparent planar waveguide. Figure 4c introduces another configuration using Lambertian diffused reflectors. These illustrations highlight the versatility of FPSC designs, accommodating various reflector types and solar cell arrangements to enhance solar energy capture and generation efficiency [75,76].

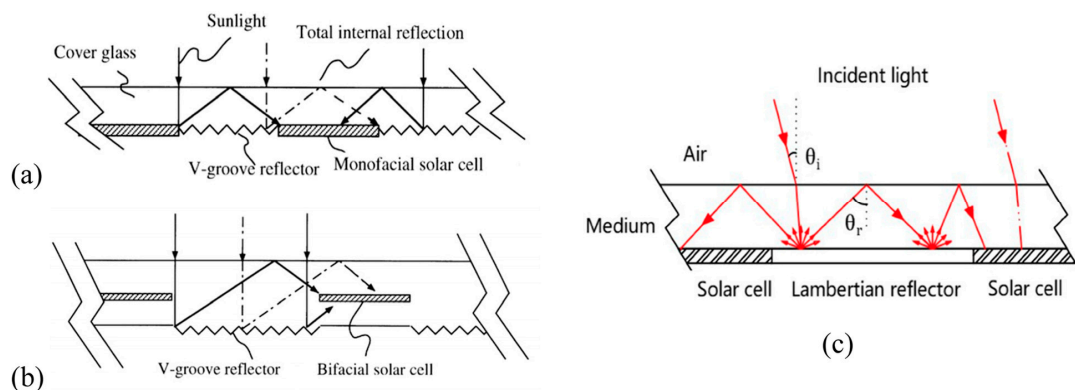


Figure 4. Cross-sectional configurations of FPSC modules with reflectors and solar cells: (a) monofacial cells with v-grooved reflectors, (b) bifacial cells with v-grooved reflectors, and (c) Lambertian diffused reflectors [75].

Figure 5 depicts a BIPV window system incorporating planar concentrating optics. In colder conditions, as depicted in the upper diagram of Figure 5a, the transparent state of the membrane allows solar radiation to penetrate, facilitating building illumination and passive heating, with a portion of the radiation reaching the front-facing solar cells. Conversely, in warmer conditions, as shown in the lower diagram of Figure 5b, the light-scattering state of the membrane redirects the scattered light toward the solar cells, enabling electricity production. This feature can aid in reducing solar heat gain and internal glare. By utilizing a thermotropic membrane composed of hydroxypropyl cellulose (HPC) and a gelling

agent such as gellan gum, the membrane not only adapts to varying weather conditions but also enhances electricity production. A sophisticated optical model incorporating Monte Carlo ray-tracing and inverse adding–doubling (IAD) techniques, was developed to examine the membrane’s angular scattering distribution under different temperatures and HPC concentrations. The model was validated using experimental data and subsequently employed to refine the design of BIPV intelligent windows. The results demonstrated that a 6 wt.% HPC membrane reduced total transmittance from 90% to 14% with increasing temperature. The prototype BIPV smart window exhibited up to 1.15 times higher short-circuit current compared to a similar system without the membrane [75].

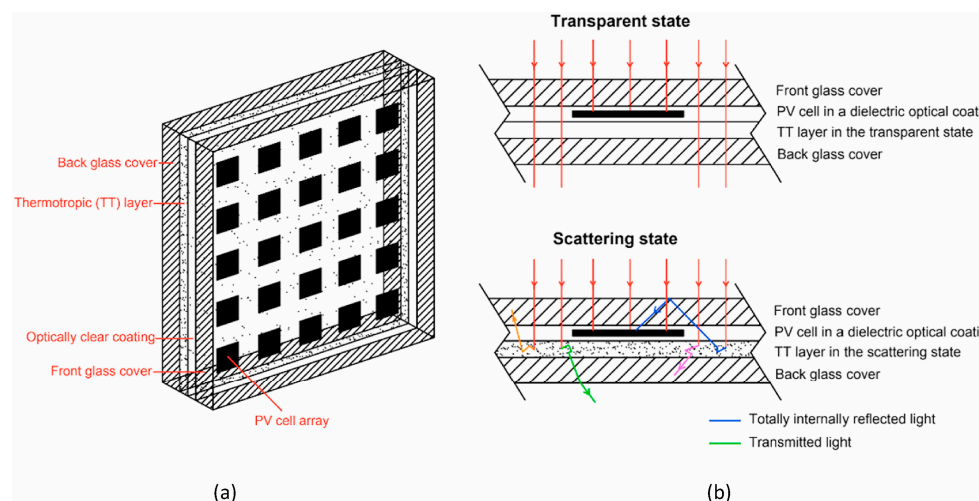


Figure 5. (a) BIPV smart window system and (b) potential light paths within the system [75].

FPSCs can be divided into three primary categories based on their optical elements: diffuse reflectors, holographic films, and LSCs. In this text, we will explore each of these categories, highlighting their features, research outcomes, and relevant references.

5.1.1. Diffused Reflectors

Diffused reflectors, particularly Lambertian-type diffused reflectors, play a crucial role in FPSCs. These reflectors evenly disperse light regardless of the angle of incidence, allowing for consistent optical concentration effects across a broad range of angles [76,77].

The smart concentrating PV system incorporates Lambertian-type diffused reflectors within its thermotropic layer, crucially influencing its operation. In Figure 6, the system’s transparent state (Figure 6b) allows sunlight transmission for daylighting and passive heating when the thermotropic layer is below its temperature threshold. Contrastingly, in the light-scattering state (Figure 6a), as the layer temperature exceeds the threshold, Lambertian reflectors scatter light within the system, enhancing sunlight redirection towards solar cells for electricity generation. Figure 7 shows a cross-sectional depiction of a non-sequential ray-tracing simulation, crucial for simulating the behavior of the smart CPV system. This simulation helps in comprehending light characteristics, particularly when the thermotropic layer functions as a Lambertian diffuse reflector, accurately predicting light scattering and reflection. By optimizing the system’s design and performance under varying temperature conditions, this approach contributes to enhancing overall energy efficiency [78]. Figure 8 demonstrates the optical efficiency of the smart CPV system regarding all-directional incidence angles. It indicates that while the lowest efficiency (around 25%) occurs at perpendicular solar rays, efficiency increases as the angle ‘ θ ’ deviates from normal incidence. This increase in efficiency is attributed to a greater amount of solar radiation reaching the solar cells directly, thus bypassing losses from reflection. Moreover, Figure 9 emphasizes the system’s performance under different solar incident angles (angle ‘ α ’ at 0),

demonstrating its advantageous angular acceptance, which is particularly useful for the diffuse solar radiation prevalent in northern European climates [78].

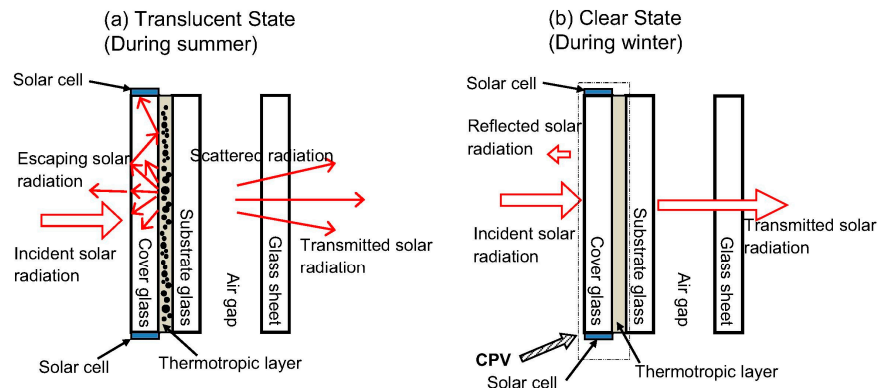


Figure 6. A cross-sectional view illustrating the operational principle of the proposed concentrated PV system [78].

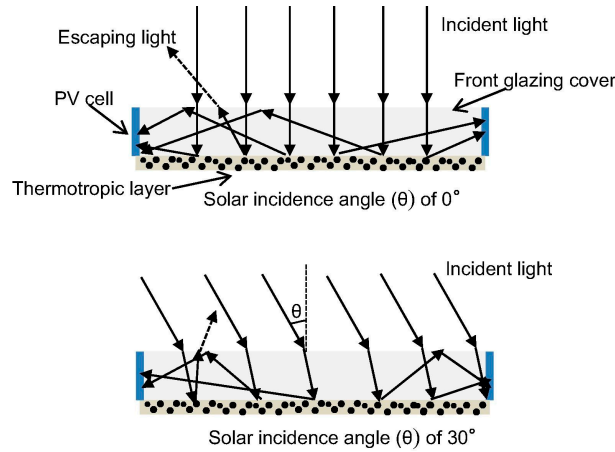


Figure 7. Non-sequential ray tracing diagram depicting the smart concentrated PV system, displaying 6 rays for each angle of incidence [78].

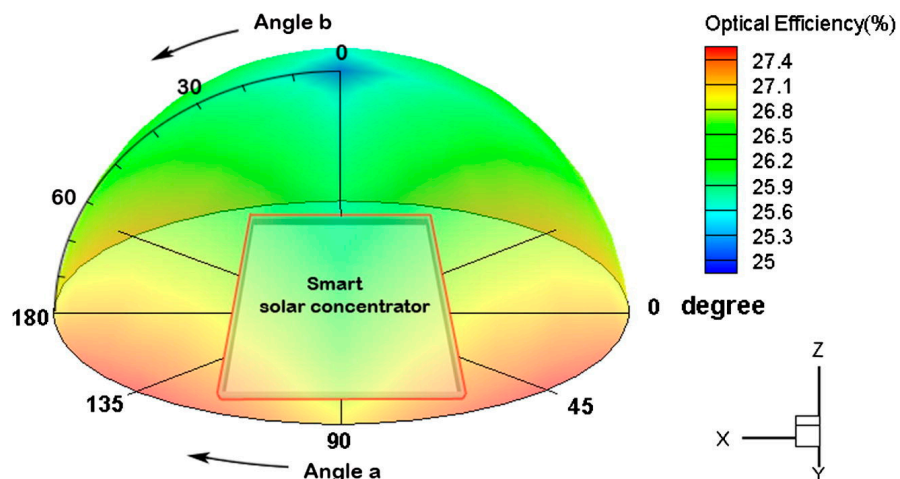


Figure 8. The optical effectiveness of the intelligent CPV under all-directional solar incident angles [78].

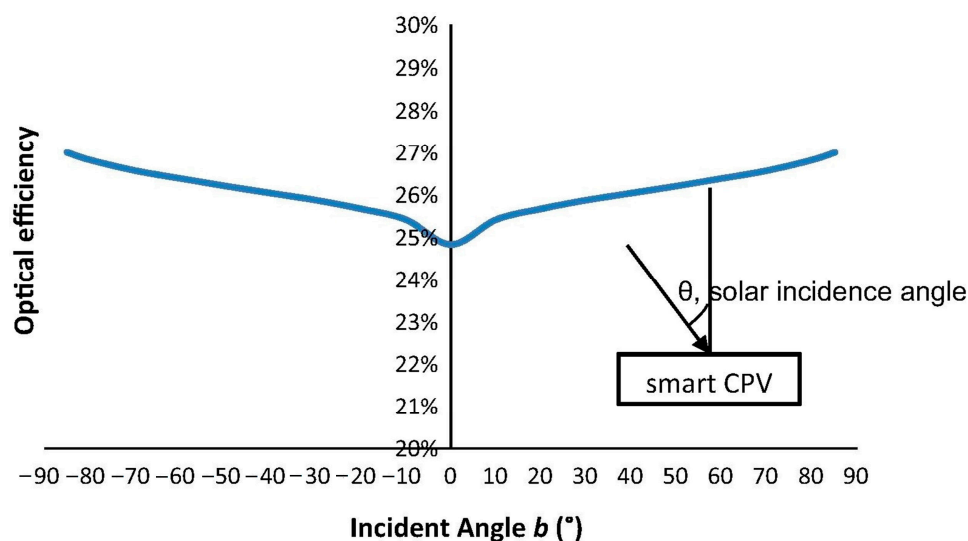


Figure 9. The optical efficiency of the intelligent CPV system at an angle of $a = 0$ [78].

It is noteworthy that the conventional ray-tracing technique may not yield accurate predictions regarding optical performance when dealing with a translucent medium, given the anisotropic nature of light reflection from such mediums [79]. In such scenarios, employing a model that incorporates non-Lambertian scattering with angular distribution becomes imperative to ensure more precise estimations [80,81].

5.1.2. Holographic Films

Holographic films, also called holographic optical elements (HOEs), are becoming a hopeful flat concentrating optic for solar energy uses, especially in BIPV setups. These slim, light films provide numerous benefits compared to traditional refractive or reflective optical elements, which makes them appealing for solar concentration and easy incorporation into building exteriors like facades or windows. By leveraging the unique properties of HOEs, this system offers the potential for enhanced efficiency, reduced cell area, spectral matching, and seamless integration with building façades [82,83].

The key components of the holographic concentrating system are two cylindrical HOEs strategically placed symmetrically on the same plane. These HOEs are designed to diffract incident sunlight towards the centrally positioned *Mono-Si* PV cell, which receives the concentrated light. The louvers are engineered to follow the solar altitude trajectory, guaranteeing that the projection of incident sunlight rays on the YZ plane (θ) remains constant at zero, while permitting variation in the angle on the XZ plane (φ). This arrangement strategically aligns the high angular selectivity direction of the HOEs with the tracking orientation (solar altitude), while positioning the low angular selectivity direction with the non-tracking orientation (solar azimuth). Furthermore, the holographic concentrating system offers the unique advantage of seamless integration with building façades, serving as both a solar energy generator and a shading element. This dual functionality not only contributes to energy savings but also enhances the overall building performance. The envisaged system is planned for integration within solar shading louvers positioned on the southern facade of buildings in the Northern Hemisphere (or on the northern facade in the Southern Hemisphere) [84].

Table 2 summarizes the key results and findings reported by various researchers on the use of HOEs in window solar applications, including theoretical and experimental efficiencies, concentration ratios, system configurations, and potential applications for building integration and shading.

Table 2. HOEs in window solar applications.

Ref.	Focus	Key Findings
[85]	Holographic PV Systems	<ul style="list-style-type: none"> Theoretical system efficiency of 41% was achieved using holographic concentrating and spectral splitting PV systems with a GaAs-InGaAs tandem cell. The prototype system demonstrated consistent efficiency over a 15-min period without a heatsink, highlighting the system's robustness. A comparative analysis with a Fresnel system indicated that the holographic system sustained superior efficiency over time. Specifically, the Fresnel system experienced a 50% reduction in efficiency within 30 s in the absence of a heatsink. The cost analysis projected that once production levels reach a capacity of 20 MW per year, the system could generate power at a cost of 5.7 cents per kWh, indicating potential cost savings compared to existing systems.
[83]	Holographic Spectrum-Splitting PV	<ul style="list-style-type: none"> A study achieved a system efficiency of 31.0% through the application of holographic spectrum-splitting optical systems incorporating transmission holographic lenses alongside GaAs and a 2.1-eV bandgap solar cell under one-sun illumination conditions. Additionally, the study demonstrated successful fabrication of high-efficiency transmission holograms in dichromated gelatin, showcasing potential advancements in PV technology.
[86]	Building-integrated Solar Innovation	<ul style="list-style-type: none"> We have suggested a building integration system that merges shading with PV power generation by focusing diffracted light onto solar cells. This system was installed on the facade of the Shell solar cell factory in Gelsenkirchen, Germany.
[87]	Sol-Gel Holographic Lenses for Concentration	<ul style="list-style-type: none"> Sol-gel-based photopolymers recorded holographic lenses with low shrinkage (2.2%), surpassing traditional materials with shrinkage values of 7–8%. Holographic lenses facilitated the creation of efficient solar concentrators with passive solar tracking, enhancing the operation of PV cells within the visible range (400–700 nm) while simplifying the design of cooling systems.
[82]	Cylindrical HOE Efficiency	<ul style="list-style-type: none"> Attained 17.9% electrical efficiency using a cylindrical HOE system with crystalline silicon cells and a 3.5× concentration ratio, indicating enhancement compared to unaided cells.
[88]	Axial HOE for Advanced augmented reality (AR)	<ul style="list-style-type: none"> The study introduces an AR glasses optical system based on axial HOE, providing a wide field of view (60°), large eyebox (10 mm), and high spectral selectivity (<12 nm). Modeling, assembly, and experimental measurements validate the system's high output characteristics, indicating its potential for integration into AR systems, despite drawbacks such as potential straylight and increased volume compared to other HOE-based AR glasses.
[89]	Hybrid Solar Energy Conversion Innovations	<ul style="list-style-type: none"> The research presents a photovoltaic/thermal system characterized by 93% optical efficiency and a customizable power output ratio. This system tackles solar intermittency issues and improves energy storage capabilities. Incorporating a PV system into an algal biofuel process substantially boosts energy production while retaining 92% of the initial algae yield. This leads to a 2.4-fold increase in energy return on investment compared to the standalone biofuel system, demonstrating its economic feasibility.
[90]	HLC system using HOE and diffusers	<ul style="list-style-type: none"> The system improved annual energy yield (AEY) by 4.5% to 3.8% with direct solar illumination and AEYIs by 4.3% to 3.6% with both direct and diffuse solar illumination.

5.1.3. Luminescent Solar

LSCs are instruments consisting of a transparent polymer or glass layer embedded with luminescent materials like organic dyes or quantum dots (QDs) [91]. These luminescent materials absorb incoming sunlight and re-emit it at a longer wavelength, and the emitted light is confined within the sheet through total internal reflection. The light is then directed towards the edges of the sheet, where it can be captured by solar cells [92].

The architectural design of LSCs is accompanied by the optical losses related to them. The visualization showcases the essential elements of an LSC, with luminophores depicted as red spheres enclosed within a lightguide plate. The diagram illustrates the optimal functioning of LSCs, where photons that have undergone downshifting are guided through total internal reflection towards the edges of the lightguide. This mechanism facilitates PV

cells in capturing the concentrated and amplified sunlight. LSCs are recognized for their uncomplicated approach to capturing, spectrally transforming, and optically amplifying solar photons, typically involving a luminescent material enclosed within a clear polymer or glass plate. This visual aid elucidates the photoluminescence mechanism and the enhanced energy efficiency facilitated by total internal reflection within LSCs [93].

The key advantage of LSCs for photovoltaic-integrated thermal windows is their ability to selectively absorb and convert specific wavelengths of light while maintaining transparency in the visible range [94]. This allows LSCs to function as power-generating window elements, contributing to energy generation while also providing daylighting and thermal insulation [95].

The target efficiencies for LSCs using ideal quantum dot (QD) luminophores are delineated for both opaque and semi-transparent devices (with an average visible transmission of 50%) as follows: (i) 11.0% and 5.5% for laboratory-scale devices; (ii) 10.0% and 5.0% for pilot-scale modules; and (iii) 9.0% and 4.5% for commercial-scale modules. It is important to note that the design requirements for QDs, particularly the overlap integral between absorption and emission spectra, become increasingly critical as LSC dimensions grow [92].

A significant characteristic of LSCs is their capacity to concentrate both direct and diffuse sunlight [96,97], making them particularly suitable for regions with substantial cloud cover, such as central Europe [98]. Moreover, LSCs can function efficiently under “cool light” conditions, which minimizes lattice thermalization losses and improves the performance of integrated solar cells [99,100].

The utilization of semi-transparent LSCs in power-generating window components holds significant potential, although opaque LSCs may face challenges in competing with traditional flat-PV modules for building integration [92]. The transition of LSCs from small laboratory-scale sizes to large commercial-scale modules presents technical obstacles such as maintaining efficiency levels, optimizing transparency, and controlling light emission direction [93,101].

Table 3 illustrates a comparative overview of LSCs with regards to their dimensions, types of luminescent materials employed, and the associated power conversion efficiencies.

Table 3. Comparative Overview of LSCs.

Ref.	LSC Size	Luminescent Species	Power Conversion Efficiency
[102]	5 cm × 5 cm	Lumogen Red & Fluorescein Yellow	7.1% (with GaAs solar cells)
[103]	60 cm × 60 cm	Lumogen Red	1.6%
[104]	150 cm × 100 cm (6 × 50 cm × 50 cm plates)	Not specified	1.3%
[105]	122 cm × 61 cm	Not specified	0.3%
[106]	30 cm × 30 cm	CuInS ₂ quantum dots	6.8% (optical power efficiency)

5.2. Non-Planar Concentrating Optics

Non-planar optical components like Fresnel lenses, wedge prisms, and CPCs are integral to BICPV glazing systems. These systems are commonly designed and optimized using ray-tracing methodologies [107].

An important issue faced by BICPV systems is their reduced transparency, attributed to the utilization of highly reflective or scattering materials necessary to achieve elevated optical concentration ratios. The adoption of dielectric material-based compound parabolic concentrators (DiCPCs) presents a practical solution for enhancing PV power generation while maintaining daylight accessibility. Various dielectric materials, such as polycarbonate [108], polyurethane [109], polymethyl-methacrylate (PMMA) [110], and Topas[®] (cyclic olefin copolymer) [108] have been studied for use in dielectric compound parabolic concentrators (DiCPCs), demonstrating high visible light transmittance levels ranging from 70% to 90% [108].

5.2.1. Fresnel Lenses

Fresnel lenses have emerged as promising non-planar concentrating optics for BICPV glazing systems. They have attracted considerable interest because of their compact structure, light weight, and capability to achieve elevated concentration ratios. Various configurations have been explored, optimizing parameters such as lens profiles, secondary optics, and solar cell sizes to enhance overall system performance. While challenges exist, such as the impact on indoor daylighting, ongoing research efforts aim to address these issues and further improve the integration and efficiency of Fresnel lens-based BICPV systems [111,112].

Fresnel linear concentrators for BICPV applications, demonstrating the effectiveness for combining linear Fresnel lenses with secondary concentrators, are discussed. The solar generator developed integrates an optical concentrator and a photovoltaic thermal absorber. By fine-tuning the optical assembly, a concentration ratio exceeding 9 is attained, channeling more than 85% of the yearly direct radiation onto the mobile solar receiver. This setup comprises a curved linear Fresnel lens serving as the primary concentrator and a compound parabolic reflector acting as the secondary concentrator. Feasibility for building integration is demonstrated with a concentration ratio between 2.5 and 10. Key achievements include optimized optical, thermal, and electrical designs, which are validated through I-V curves and numerical thermal analysis. The system functions within a Reynolds number span of 200–250, maintaining a temperature difference exceeding 6 °C and a PV cell temperature at approximately 55 °C, with a Nusselt number of approximately 7 [113].

A proposed BICPV system integrates a Fresnel lens concentrator as a secondary optical element (SOE) along with a highly efficient triple-junction solar cell. The system components, including a secondary concentrator designed to improve light reception efficiency, are illustrated in Figure 10. The concentrator, made of K9 glass with excellent optical transmittance, had specific dimensions of 12 mm (upper opening), 5.35 mm (lower opening), and 20 mm (height). The system achieved efficiencies of up to 40% within a temperature range of −40 °C to 100 °C, with a maximum operational temperature of 180 °C. Simulation and experimental results indicated an optical efficiency of 86.5% and a geometric concentration ratio of 1000 suns, with a wide acceptance angle of $\pm 1.2^\circ$ suitable for building integration [114].

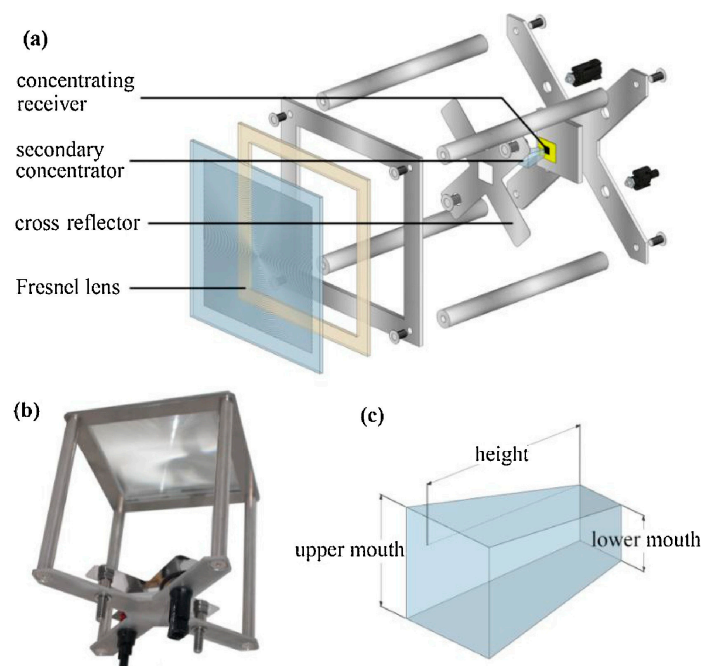


Figure 10. Integrated concentrating module design of Fresnel lenses: (a) the main components of the concentrating module, (b) real model, (c) secondary optical element (SOE) [114].

In addition to electricity generation, heating and cooling contributions can be made by BICPV systems incorporating Fresnel lenses into buildings. The integration of a Fresnel lens solar collection system into a building facade to meet apartment heating needs was evaluated, and energy savings were analyzed. The suggested system was found to save 16% in the Dutch climate compared to a conventional modulating boiler with the same heat pump. Savings of 43% were observed compared to the boiler directly connected to floor heating [115].

Balancing energy production and visual comfort is important when BICPV systems are integrated into buildings. The quality of daylight can be improved by adjusting the thickness of the integrated PV modules [116]. An optimal equilibrium can be attained by semi-transparent PV systems that strike a balance between decreasing energy usage, enhancing power generation, and mitigating glare. These systems typically have a transparency level ranging from 20% to 30% [117].

5.2.2. Prismatic Lenses

Prismatic lenses utilizing total internal reflection (TIR) have surfaced as a compelling non-planar concentrating optical solution for BICPV glazing systems. They provide a distinct advantage by concentrating direct solar radiation onto PV cells while permitting diffuse solar radiation to penetrate into the building interior. This dual functionality enhances both energy generation and daylighting within buildings. The suggested design of a building facade, depicted in Figure 11, illustrates transparent acrylic segments arranged in a prismatic pattern, along with the integration of solar cells onto these segments [118].

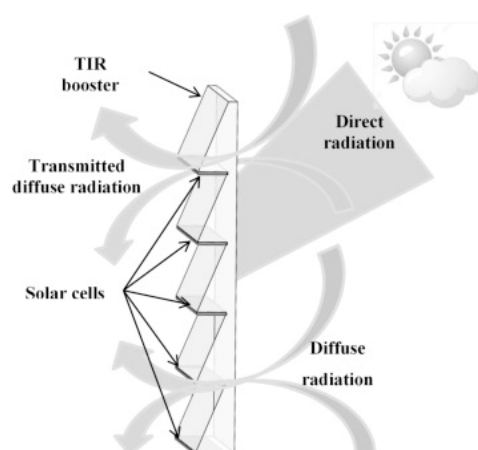


Figure 11. Proposed prismatic façade design [118].

Prismatic solar concentrators, which exploit TIR within materials of high refractive index, underwent extensive study to enhance their efficiency and performance for building-integrated solar applications [119,120]. The development of low-concentration static prism concentrators (prism CPV modules) aimed to reduce costs by substituting expensive solar cells with more affordable concentrators made of plastic and glass [121,122].

However, challenges such as incident angle dependency were deemed crucial. This dependency necessitated adjustments in the geometry of prism CPV modules to optimize performance across different latitudes and tilt angles. In response, their methodology expanded the angular range of optical efficiency for prism concentrators, leading to notable enhancements in performance across different sunlight conditions. Additionally, they developed a transparent prism CPV module by integrating a low-concentration prism concentrator with PV cells. Through thorough ray-tracing analysis and field experiments, they illustrated that the prism concentrator efficiently directed direct solar radiation onto the PV cells while enabling diffuse radiation to enter the building interior [123].

Sophisticated ray-tracing simulations were utilized to implement a low-concentration, PV-integrated prismatic segmented façade aimed at effectively capturing direct normal

irradiance (DNI) incident on these specific façade configurations, particularly during summer periods. Different prismatic TIR façade segments were employed, each with different head angles ranging from 17° to 25° . Façades featuring smaller head angles effectively captured radiation in more concentrated intervals around midday, whereas those with larger head angles efficiently gathered DNI throughout the day, demonstrating adaptability in energy capture strategies [118].

5.2.3. Compound Parabolic

Dielectric-based CPCs offer promising solutions for BIPV applications, enabling improved power generation and daylighting capabilities. Researchers have explored various geometrical designs and dielectric materials to optimize optical efficiency, acceptance angles, and temperature management. While challenges remain, such as high solar cell temperatures and non-uniform illumination, ongoing research efforts aim to address these issues and facilitate the widespread adoption of dielectric-based compound parabolic concentrators (DiCPCs) in BIPV systems [124,125]. The fundamental geometry of a compound parabolic concentrator (CPC), depicted in Figure 12, consists of two parabolic reflecting surfaces that concentrate sunlight onto a target surface [126,127].

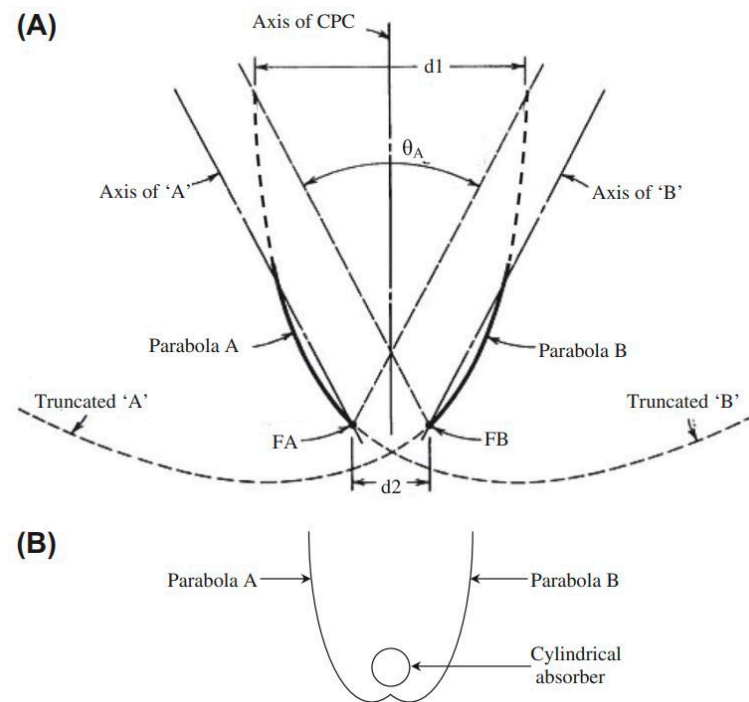


Figure 12. The basic geometry of 2D CPC, (A) The conventional geometry, (B) Schematic of CPC with cylindrical absorber [127].

Researchers have explored various geometrical configurations of DiCPCs, including three-dimensional crossed CPC [109,110], rotational asymmetric CPC [128], linear asymmetric CPC [129,130], and lens-walled CPC [131], with the goal of improving optical efficiency, current–voltage (I–V) characteristics, and temperature distribution, as summarized in Table 4.

One notable example involves the use of 3D crossed compound parabolic concentrators (3DCCPCs), made from transparent polyurethane (Crystal-clear 200[®], AMT Composites, Johannesburg, South Africa) and attached for solar cells utilizing encapsulation material (Sylguard-184, Dow Inc., Midland, MI, USA). Simulations indicated an acceptance half-angle of 34.5° and a peak optical efficiency of 73.4%. Compared to a non-concentrating setup under normal light conditions, the CPV system exhibited a maximum power output 2.65 times higher [109,132].

The asymmetric compound parabolic concentrators (ACPCs) developed by the University of Exeter team allowed for efficient light collection within the acceptance angle range of 0–55° while also permitting daylighting. Testing indoors revealed that under a 20° angle of incidence, the system reached a peak optical efficiency of 80.5% and a maximum power ratio of 2.27 compared to a non-concentrating configuration [133,134].

The PV facades of reduced costs incorporating devices with optically concentrating elements (PRIDE) technology, featuring 3 mm and 9 mm wide single-crystal silicon solar cells, exhibited enhanced power generation capabilities compared to non-concentrating systems. Indoor characterization using flash and continuous solar simulators highlighted this advantage. However, long-term characterization revealed durability issues with the dielectric material when using casting technology [135].

Table 4. Dielectric-based compound parabolic concentrators (DiCPCs).

Ref	DiCPC Design	Concentration Ratio	Acceptance Half-Angle	Maximum Optical Efficiency	Maximum Power Ratio/Increment
[109]	3D Crossed CPC (3DCCPC)	-	34.5°	73.4%	2.65× higher than non-concentrating
[133]	Linear Asymmetric CPC (ACPC)	2.8×	0–55°	80.5%	2.27× higher at 20° incidence
[135]	Linear Asymmetric CPC (ACPC)	2×	0–66°	10.5% electrical conversion efficiency	62% increase in max power
[136]	absorptive/reflective CCPC (AR-CCPC)	3.6× to 4×	4.65°	91%	2.84× compared with the bare solar cell
[137]	Dielectric Asymmetric CPC (DACPC)	2.4×	-	93.3% (sim), 77.9% (exp)	96.6% increase in max power, 87% increase in I_{sc} (0–85°)

Introducing absorptive/reflective CCPC (AR-CCPC), a novel CPV concept derived from CCPC. AR-CCPC's optical, thermal, and total efficiency were simulated using APEX software (version 5.03), comparing concentration ratios from 3.6 to 4. Results favored the 3.6 CCPC for solar cell efficiency and incident tolerance. The 3.6/4 AR-CCPC showed superior overall optical efficiency across all angles. A basic thermal model without water flow indicated an increased wall temperature with added thermal absorbents. Experimental results aligned with simulations, promising enhancements for solar concentrator systems. AR-CCPC's potential for combined thermal and electricity generation in integrated systems was highlighted, paving the way for practical PV/T hybrids [136].

Despite the substantial increase in power generation, the use of dielectric CPCs often results in elevated temperatures in solar cells and uneven light distribution across their surface. Analysis and monitoring of the thermal and electrical performance of a linear ACPC setup revealed a peak temperature rise of 51 °C in the solar cells, leading to a decline in power conversion efficiency from 18.5% (at 23 °C) to 15.6% (at 74 °C) [107]. The uneven flux distribution across the solar cell surface can lead to negative effects such as hot spots, current imbalances, and a decline in cell performance [107,113].

A systematic design methodology was proposed for asymmetric CPCs, focusing on achieving a desired angular acceptance range. The resultant dielectric asymmetrical compound parabolic concentrator (DACPC) exhibited near-optimal angular acceptance efficiency. Ray-tracing simulations and practical evaluations showed that the DACPC, with a geometric concentration ratio of 2.4, enhanced the short-circuit current and maximum power output by 87.0% and 96.6%, respectively, within an incident angle range of 0–85°, compared to a non-concentrating PV cell. The average optical efficiencies from simulations and real-world tests were 93.3% and 77.9%, respectively. The efficiency of angular acceptance, vital for evaluating yearly performance and local suitability, peaked at 97.7% in simulations and 94.4% in experiments [137].

To address the overheating problem, researchers have proposed integrating concentrated photovoltaic (CPV) systems with passive cooling techniques such as natural ventilation and PCMs [26,138]. Nevertheless, these remedies pose challenges in terms of expenses and intricacy in architectural amalgamation.

6. Thermotropic Smart Glazing Technologies

Thermotropic smart glazing technologies provide an innovative method for dynamically managing solar heat gain and daylighting within buildings. This is achieved by integrating thermotropic materials into window systems. These materials exhibit a reversible change in optical properties, particularly light transmittance, in response to temperature variations.

The core working mechanism lies in thermotropic hydrogels, which are water-based polymer networks containing both hydrophilic and hydrophobic groups. When the temperature is below the lower critical solution temperature (LCST), which is generally in the range of 25–35 °C, the hydrophilic polymer chains are soluble in water, leading to a transparent hydrogel state. As the temperature exceeds the LCST, the polymer chains undergo a phase change, gathering together and pushing out water molecules. This phase transition induces light scattering at the boundaries between the polymer-rich and water-rich areas, resulting in the hydrogel appearing translucent or opaque [139,140].

Extensive research has been conducted on both synthetic polymers, like poly(N-isopropylacrylamide) PNIPAm, (N-isopropylacrylamide)-2-aminoethylmethacrylate hydrochloride) PNIPAm-AEMA, and biopolymers, such as HPC, for developing thermotropic hydrogels with desirable optical properties and transition temperatures. Various strategies, including copolymerization, addition of co-solvents, and salt inclusion, have been employed to tune the LCST and optical performance [141,142].

Table 5 provides an overview of the optical characteristics of specific thermotropic hydrogels, outlining their capacity for modulating visible transmittance (ΔT_{lum}), near-infrared transmittance (ΔT_{IR}), and solar transmittance (ΔT_{sol}).

Table 5. Optical performance of thermotropic hydrogels.

Ref.	Hydrogel	Thickness	ΔT_{lum}	ΔT_{IR}	ΔT_{sol}
[143]	PNIPAm	78 μm	65.9%	31.7%	49.6%
[144]	PNIPAm-AEMA	240 μm	87.2%	75.6%	81.3%
[142]	HPC-gellan gum	-	~80% (at 600 nm)	-	-

Diverse approaches have been investigated to adjust the optical qualities and transition temperatures of thermotropic hydrogels, encompassing copolymerization, incorporation of co-solvents, and salt integration. For instance, PNIPAm hydrogels can be customized to display lower critical solution temperature (LCST) values varying between 25 °C and 40 °C through copolymerization with either hydrophobic or hydrophilic monomers [145]. The LCST of PNIPAm hydrogels could be decreased from 32.2 °C to 20.4 °C by increasing the glycerol concentration from 0 wt.% to 35 wt.% in the water-glycerol solvent blend [141]. Moreover, the inclusion of glycerol co-solvent not only improved the freezing resilience of PNIPAm hydrogels but also reduced water evaporation.

Regarding biopolymer-based hydrogels, HPC-based thermotropic hydrogels with varying polymer and gelling agent concentrations are shown in Table 6. Higher HPC concentrations resulted in lower transmittance and higher reflectance in the translucent state above the transition point (~42 °C), demonstrating the ability to control the light-scattering performance [142].

Table 6. Optical properties of HPC-gellan gum hydrogels at 60 °C [142].

HPC (wt.%)	Gellan Gum (wt.%)	Transmittance (600 nm)	Reflectance (600 nm)
6	1.5	~20%	~50%
4	1.2	~40%	~35%
2	0.8	~60%	~25%

Moreover, the addition of salts has been shown to shift the cloudy point (phase separation temperature) of HPC aqueous solutions. Heightening the sodium chloride (NaCl) concentration from 0 to 1.4 mol/L, for instance, triggered a decrease in the clouding point of HPC solutions from 42 °C to 20 °C [146].

Incorporating thermotropic hydrogels into window systems shows significant promise in enhancing building energy efficiency and indoor environmental conditions. HPC-based thermotropic windows, for example, delivered up to 22% annual energy savings in a Mediterranean climate due to decreased cooling demands. Additionally, a smart window system covering a large area (1 m²) and utilizing a PNIPAm-based thermotropic hydrogel achieved a 45% decrease in HVAC energy usage compared to standard double glazing in Singapore’s climate [147].

To enhance the efficiency of thermotropic windows, a window structure known as thermotropic parallel slat-transparent insulation material (TT PS-TIM) has been developed, as depicted in Figure 13. This system merges thermotropic substances with insulating slats to provide dynamic control over solar heat gain and daylight infiltration while boosting thermal insulation. Simulations carried out for various climates (London, Stockholm, Rome, and Singapore) indicated that the TT PS-TIM system could yield energy savings of up to 21.5% compared to standard double glazing, alongside improved access to daylight [148,149].

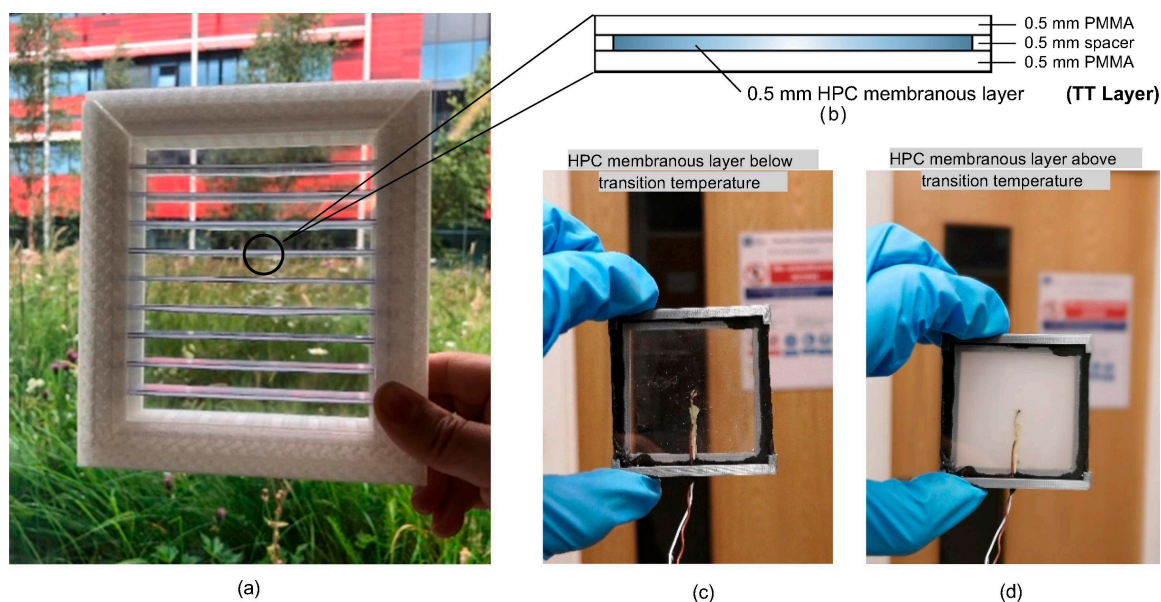


Figure 13. (a) the TT PS-TIM window model, (b) slat design schematic, (c) HPC membrane below transition temperature, and (d) HPC membrane above transition temperature [148].

Adjusting the optical properties and transition temperature of the thermotropic material layer is crucial to achieve a balance between energy efficiency and daylight provision. They noted that reducing absorbance in the translucent state could decrease energy usage while aiming for a lower transition temperature, approximately 21 °C for the London climate, which could enhance daylight performance. Furthermore, they proposed varying optimized designs tailored to different climatic conditions [149].

Table 7 summarizes the energy-conserving abilities and daylight performance of distinct TT PS-TIM window prototypes tailored for London’s climate. The table outlines different prototypes along with their corresponding transition temperatures ($^{\circ}\text{C}$), energy-saving potential, and average UDI 500–2000 lx values. The prototypes are labeled as CS-TSt followed by their transition temperature and optical characteristics, with “r” indicating reflectance and “T” representing transmittance in the visible spectrum. For example, the CS-TSt40r35 prototype, featuring a transition temperature of 35°C , demonstrates an energy-saving potential of 21.7% and an average UDI 500–2000 lx value of 67.1%. Similarly, other prototypes such as CS-TSt20r35, CS-TSt10r35, and CS-TSt10r19 exhibit varying energy-saving potentials and average UDI values, providing insights into the performance variations based on different design parameters [149].

Table 7. Energy and daylighting efficacy of TT PS-TIM windows in London’s climatic conditions [149].

Prototype	Transition Temp. ($^{\circ}\text{C}$)	Energy Saving Potential	Average UDI 500–2000 lx *
CS-TSt40r35	35	21.7%	67.1%
CS-TSt20r35	35	21.2%	69.8%
CS-TSt10r35	35	20.7%	72.2%
CS-TSt10r19	19	19.8%	74.4%

* Indicates the mean effective daylight illumination (UDI) level ranging from 500 to 2000 lx delivered by each model.

7. Technologies in Dynamic Glazing for the Purposes of Generating Electricity and Managing Daylight

The integration of smart window technology with BIPV windows has given rise to an emerging area of study referred to as BIPV smart window. In recent times, innovative concepts have emerged by merging partially see-through PV systems with optically changeable materials.

Switchable PV-electrochromic (PV-EC) glazing technology, which combines PV-EC glazing, is viewed as a forward-looking solution for creating energy-efficient and environmentally friendly buildings. Theoretical models for windows incorporating PV-EC technology were developed as feasible architectural solutions [150,151]. This process entailed a comparative evaluation of three PV-EC technologies: side-by-side (SBS) technology, tandem solid technology (TST), and tandem liquid technology (TLT). The evaluation considered functional aspects such as thermal and visual comfort, energy efficiency, and aesthetics, thus outlining the advantages and disadvantages of each technology. From this analysis, seven window models were devised, showcasing the potential of effectively combining PV and EC technology. Recommendations were made for PV-EC glazing configurations for building facades, with a focus on insulated facades in moderate climates, highlighting the importance of thermal protection while maintaining a visually pleasing environment. Table 8 offers a comparative evaluation of three varieties of switchable PV-EC glazing technologies [152].

Table 8. Comparative assessment of architectural and construction applications for PV-EC technologies: SBS, TST, and TLT [152].

Aspects	SBS	TST	TLT
Thermal Comfort	- It is appropriate for solar control glazing, although a gradual phase transition might necessitate supplementary assistance. The PV elements offer enduring solar control measures.	- In colder regions characterized by ample sunshine, the sluggish phase transition renders it less effective for solar control	- Higher and faster phase transition than TST, making it more suitable as solar glazing.

Table 8. Cont.

Aspects	SBS	TST	TLT
Visual Comfort	<ul style="list-style-type: none"> - It offers versatility in managing both EC-PV systems for lighting control purposes. Additionally, it serves as a regulator for light access by maintaining visual contact with the surroundings. 	<ul style="list-style-type: none"> - Problems with transparency and color uniformity. - Low Tv values limiting daylight access. 	<ul style="list-style-type: none"> - It presents enhanced characteristics in contrast to TST, making it suitable for spaces that need both natural light and glare mitigation. However, the stripes may distort visual connection with the surroundings more than the insulating elements in TST.
Energy Efficiency	<ul style="list-style-type: none"> - Flexibility in configurations optimizes protection against overheating. - Lowest risk of damage. - Greater possibilities in selecting PV technology. 	<ul style="list-style-type: none"> - Provides protection against overheating, but reduces daylight access. - Most complex structure with potential damage risks. - Limited PV usage. 	<ul style="list-style-type: none"> - Similar to TST but with higher Tv values, reducing artificial lighting. - Less complicated structure with lower risk of damage.

An innovative photothermally controlled PV window has been introduced, boasting remarkable features suitable for both power generation and daylight management. This innovative technology provides a high level of visible light transmission, achieving 68%, along with an impressive power conversion efficiency of up to 11.3% and a rapid switching time of less than 3 min. The crucial element enabling its operation is the switchable absorbing layer consisting of a methylammonium lead iodide-methylamine complex ($\text{CH}_3\text{NH}_3\text{PbI}_3 \cdot x\text{CH}_3\text{NH}_2$). This layer's capability to form or dissociate allows the PV window to transition between a clear state with 63% visible light transmission and a tinted state with 3% visible light transmission, providing flexibility in light management. The transition process is influenced by the CH_3NH_2 gas partial pressure and the temperature of the $\text{CH}_3\text{NH}_3\text{PbI}_3 \cdot x\text{CH}_3\text{NH}_2$ solid. In its transparent state, the PV window remains colorless; however, when exposed to sunlight, it undergoes a significant color transformation, leading to a notable increase in short-circuit current density, reaching up to 21.2 mA/cm^2 under standard conditions (1000 W/m^2 , AM1.5). This technology effectively resolves the traditional trade-off between the high visible light transmission and efficient power conversion encountered in semi-transparent PV systems. Nonetheless, it is crucial to note that prolonged usage may lead to performance decline due to degradation or structural alterations in the $\text{CH}_3\text{NH}_3\text{PbI}_3$ layer [153].

Numerous methods have been investigated to improve the capabilities of smart windows in managing daylight and generating electricity. An example of an approach involves the development of a self-powered smart window using PDLC, which achieves 41% visible light transmittance in the OFF state and 68% in the ON state [154]. A smart window incorporating a VO₂-based thermochromic film demonstrated modest power conversion efficiencies of only up to 0.52% [155]. The integration of an HPC-based thermotropic reflective layer into BIPV windows yielded an optical efficiency of 10% and a concentration ratio of 0.5 [78]. PV thermochromic smart windows with LCS temperatures ranging from 20 °C to 40 °C achieved solar energy modulations of up to 76% and exhibited a 12% enhancement in power output compared to conventional crystalline silicon PV glazing [156–159]. Table 9 provides a summary of key performance parameters in selected BIPV smart window technologies.

Table 9. Performance of BIPV smart window technologies.

Reference	Technology	Visible Light Transmittance	Power Conversion Efficiency	Solar Energy Modulation
[153]	Photothermally modulated PV	Up to 68%	Up to 11.3%	-
[151]	PV-EC	Adjustable (0–3.5 V)	-	-
[154]	PV-PDLC	41% (OFF), 68% (ON)	-	Limited
[155]	PV-VO2	-	Up to 0.52%	-
[156–159]	PV-TT	-	Up to 12% higher than c-Si PV	Up to 76%

8. Solar Windows and Solar Protection on Building Performance

Solar windows, also known as LSCs, are an innovative technology that can serve dual purposes: generating electricity from sunlight and providing solar protection for buildings. The use of solar protection strategies, including specialized glazing, can significantly affect both the thermal and lighting performance of buildings. These strategies aim to balance the need for natural daylight with the requirement to reduce solar heat gain, especially in climates with hot summers [160].

Window design plays a crucial role in energy efficiency and functionality. Factors such as window area, proportions, position, external shading, and glazing properties all impact heating, cooling, and lighting needs [161]. The integration of daylight with artificial lighting systems can lead to substantial energy savings, varying based on room dimensions, geographic location, and external illuminance levels [162].

Interestingly, a study on red LSCs (similar to solar windows) found that covering 25% of a window with an LSC was judged favorably by participants compared to a normal, clear glass window. This suggests that solar windows could potentially improve both energy efficiency and occupant well-being [163].

Building codes often require a balance between energy efficiency and occupant comfort. Window parameters such as U-value, SHGC, and visible transmittance (T_{vis}) are essential factors in meeting these requirements [40]. The WWR also plays a significant role in determining interior temperature, energy consumption, and CO₂ emissions [164].

Table 10 summarizes the multifaceted effects of solar windows and solar protection technologies on building performance, including their influence on interior lighting conditions, building code compliance, occupant comfort, and environmental impact, based on findings from various studies.

Table 10. Impact of solar windows and solar protection on building performance.

Reference	Visible Light Transmittance	Aspect
[160]	Can reduce excessive daylight while still allowing natural light.	Lighting Conditions PV-PDLC
[163]	Can potentially improve occupant well-being.	
[40]	Assists in meeting requirements for SHGC.	Building Code Compliance
	Contributes to achieving desired visible transmittance (T_{vis}).	
[164]	Helps in managing WWR effects.	Occupant Comfort
[164]	Can reduce discomfort hours related to temperature.	
[163]	May be perceived favorably by occupants (when covering 25% of a window).	
[164]	Can reduce CO ₂ emissions by about 22%.	Environmental Impact

9. Discussion and Conclusions

This comprehensive review has unveiled a myriad of innovative BIPV glazing solutions that seamlessly integrate with smart window technologies, enabling remarkable

strides toward energy efficiency and daylighting control in buildings. These state-of-the-art technologies fall into three main categories depending on their primary functions: concentrating PV glazing, thermotropic smart glazing, and dynamic glazing systems that integrate BIPV with smart window features.

BICPV glazing systems have demonstrated exceptional performance by leveraging various concentrating optics to boost the efficiency of integrated PV cells while facilitating controlled daylighting transmission. Significant breakthroughs have been achieved in planar concentrating optics, such as diffused reflectors, holographic films, and LSCs, as well as non-planar optics like Fresnel lenses, prisms, and CPCs. Notably, a BICPV system incorporating a Fresnel lens concentrator achieved an optical efficiency of up to 86.5% and an impressive geometric concentration ratio of 1000 suns. Holographic concentrating systems employing transmission holographic lenses and GaAs/2.1-eV bandgap tandem solar cells attained a remarkable 31.0% system efficiency under one-sun illumination. LSCs employing optimal quantum dot luminophores demonstrated ambitious yet attainable target efficiencies of 11.0% and 5.5% for laboratory-scale devices with opaque and semi-transparent (50% visible transmission) configurations, respectively.

Thermotropic smart glazing systems utilizing the distinctive characteristics of thermochromic hydrogels have demonstrated impressive energy-saving abilities by dynamically controlling solar heat gain and daylight transmission based on temperature fluctuations. An exemplary instance is a PNIPAm-based thermotropic window system covering a significant area (1 m²), which managed to reduce HVAC energy consumption by 45% when contrasted with standard double glazing in Singapore's tropical climate. Additionally, the TT PS-TIM window system exhibited energy savings of up to 21.5% compared to double-glazing in various climates like London, Stockholm, Rome, and Singapore, all while improving the availability of daylight.

Emerging dynamic glazing technologies have successfully integrated BIPV functionality with smart window capabilities, resolving the trade-off between high visible light transmission and efficient power conversion. These systems offer the unique advantage of simultaneous electricity generation and daylight regulation within a single glazing unit. A photothermally controlled methylammonium lead iodide PV window exhibited an outstanding 68% visible light transmission, coupled with an impressive 11.3% power conversion efficiency and a rapid switching time of less than 3 min. PDLC smart windows achieved visible light transmittance ranging from 41% in the OFF state to 68% in the ON state, with self-powered operation enabled by integrated PV cells.

Furthermore, switchable PV-EC glazing technologies, such as SBS, TST, and TLT configurations, have demonstrated promising thermal and visual comfort, energy efficiency, and aesthetic potential. The TLT technology, in particular, exhibited higher and faster phase transition compared to TST, making it more suitable for solar control glazing in various climatic conditions.

These innovative BIPV glazing and smart window technologies hold transformative potential for establishing sustainable and energy-efficient built environments, significantly contributing to global initiatives aimed at mitigating climate change and promoting environmental sustainability. By seamlessly integrating PV energy generation with dynamic thermal regulation and daylighting control, these glazing systems offer a game-changing solution for reducing energy consumption and carbon footprint in buildings.

Author Contributions: Conceptualization, M.G. and S.S.; methodology, M.G.; validation, M.G. and S.S.; formal analysis, S.S.; investigation, M.G.; resources, S.S.; data curation, M.G.; writing—original draft preparation, M.G.; writing—review and editing, S.S.; visualization, M.G.; supervision, S.S.; project administration, S.S.; funding acquisition, S.S. All authors have read and agreed to the published version of the manuscript.

Funding: This research received no external funding.

Conflicts of Interest: The authors declare no conflict of interest.

References

1. Omole, F.O.; Olajiga, O.K.; Olatunde, T.M. Sustainable urban design: A review of eco-friendly building practices and community impact. *Eng. Sci. Technol. J.* **2024**, *5*, 1020–1030. [[CrossRef](#)]
2. Nabiyeu, M.; Salimov, O.; Khotamov, A.; Akhmedov, T.; Nasriddinov, K.; Abdurakhmanov, U.; Raximov, R.; Khalimov, A.; Abobakirov, A. Effect of External Air Temperature on Buildings and Structures and Monuments. *E3S Web Conf.* **2024**, *474*, 03011. [[CrossRef](#)]
3. Zhou, Y.; Ma, M.; Tam, V.W.Y.; Le, K.N. Design Variables Affecting the Environmental Impacts of Buildings: A Critical Review. *J. Clean. Prod.* **2023**, *387*, 135921. [[CrossRef](#)]
4. Yang, T.; Athienitis, A.K. A Review of Research and Developments of Building-Integrated Photovoltaic/Thermal (BIPV/T) Systems. *Renew. Sustain. Energy Rev.* **2016**, *66*, 886–912. [[CrossRef](#)]
5. Yu, G.; Yang, H.; Luo, D.; Cheng, X.; Ansah, M.K. A Review on Developments and Researches of Building Integrated Photovoltaic (BIPV) Windows and Shading Blinds. *Renew. Sustain. Energy Rev.* **2021**, *149*, 111355. [[CrossRef](#)]
6. Li, Y.; He, J. Evaluating the Improvement Effect of Low-Energy Strategies on the Summer Indoor Thermal Environment and Cooling Energy Consumption in a Library Building: A Case Study in a Hot-Humid and Less-Windy City of China. *Build. Simul.* **2021**, *14*, 1423–1437. [[CrossRef](#)]
7. Hu, M.; Qiu, Y. A Comparison of Building Energy Codes and Policies in the USA, Germany, and China: Progress toward the Net-Zero Building Goal in Three Countries. *Clean. Technol. Environ. Policy* **2019**, *21*, 291–305. [[CrossRef](#)]
8. Löschel, A. European Green Deal und Deutsche Energiewende Zusammen Denken! *Wirtschaftsdienst* **2020**, *100*, 78–79. [[CrossRef](#)]
9. Bosu, I.; Mahmoud, H.; Ookawara, S.; Hassan, H. Applied Single and Hybrid Solar Energy Techniques for Building Energy Consumption and Thermal Comfort: A Comprehensive Review. *Sol. Energy* **2023**, *259*, 188–228. [[CrossRef](#)]
10. Maghrabie, H.M.; Elsaid, K.; Sayed, E.T.; Abdelkareem, M.A.; Wilberforce, T.; Olabi, A.G. Building-Integrated Photovoltaic/Thermal (BIPVT) Systems: Applications and Challenges. *Sustain. Energy Technol. Assess.* **2021**, *45*, 101151. [[CrossRef](#)]
11. Chen, S.; Zhang, G.; Xia, X.; Setunge, S.; Shi, L. A Review of Internal and External Influencing Factors on Energy Efficiency Design of Buildings. *Energy Build.* **2020**, *216*, 109944. [[CrossRef](#)]
12. Belussi, L.; Barozzi, B.; Bellazzi, A.; Danza, L.; Devitofrancesco, A.; Fanciulli, C.; Ghellere, M.; Guazzi, G.; Meroni, I.; Salamone, F.; et al. A Review of Performance of Zero Energy Buildings and Energy Efficiency Solutions. *J. Build. Eng.* **2019**, *25*, 100772. [[CrossRef](#)]
13. Hemaida, A.; Ghosh, A.; Sundaram, S.; Mallick, T.K. Evaluation of Thermal Performance for a Smart Switchable Adaptive Polymer Dispersed Liquid Crystal (PDLC) Glazing. *Sol. Energy* **2020**, *195*, 185–193. [[CrossRef](#)]
14. Tällberg, R.; Jelle, B.P.; Loonen, R.; Gao, T.; Hamdy, M. Comparison of the Energy Saving Potential of Adaptive and Controllable Smart Windows: A State-of-the-Art Review and Simulation Studies of Thermo-chromic, Photochromic and Electrochromic Technologies. *Sol. Energy Mater. Sol. Cells* **2019**, *200*, 109828. [[CrossRef](#)]
15. Chen, F.; Wittkopf, S.K.; Khai Ng, P.; Du, H. Solar Heat Gain Coefficient Measurement of Semi-Transparent Photovoltaic Modules with Indoor Calorimetric Hot Box and Solar Simulator. *Energy Build.* **2012**, *53*, 74–84. [[CrossRef](#)]
16. Rana, M.J.; Hasan, M.R.; Sobuz, M.H.R. An Investigation on the Impact of Shading Devices on Energy Consumption of Commercial Buildings in the Contexts of Subtropical Climate. *Smart Sustain. Built Environ.* **2022**, *11*, 661–691. [[CrossRef](#)]
17. Jägerbrand, A.K. Synergies and Trade-Offs between Sustainable Development and Energy Performance of Exterior Lighting. *Energies* **2020**, *13*, 2245. [[CrossRef](#)]
18. Gao, Y.; Luo, S.; Jiang, J.; Rong, Y. Environmental-Thermal-Economic Performance Trade-off for Rural Residence Retrofitting in the Beijing–Tianjin–Hebei Region, Northern China: A Multi-Objective Optimisation Framework under Different Scenarios. *Energy Build.* **2023**, *286*, 112910. [[CrossRef](#)]
19. Dabbagh, M.; Krarti, M. Energy Performance of Switchable Window Insulated Shades for US Residential Buildings. *J. Build. Eng.* **2021**, *43*, 102584. [[CrossRef](#)]
20. Zhang, W.; Sun, Y.; Lin, Z. Coupled Evaluation of the Optical-Thermal-Electrical Performance of Customized Building-Integrated Photovoltaic Components. *Renew. Energy* **2024**, *223*, 119994. [[CrossRef](#)]
21. Singh, D.; Chaudhary, R.; Karthick, A. Review on the Progress of Building-Applied/Integrated Photovoltaic System. *Environ. Sci. Pollut. Res.* **2021**, *28*, 47689–47724. [[CrossRef](#)] [[PubMed](#)]
22. Mandalaki, M.; Tsoutsos, T. *Solar Shading Systems: Design, Performance, and Integrated Photovoltaics*; Springer International Publishing: Cham, Switzerland, 2020; ISBN 978-3-030-11616-3.
23. Suraparaju, S.K.; Samykano, M.; Dhivagar, R.; Natarajan, S.K.; Ghazali, M.F. Synergizing Environmental and Technological Advances: Discarded Transmission Oil and Paraffin Wax as a Phase Change Material for Energy Storage in Solar Distillation as a Step towards Sustainability. *J. Energy Storage* **2024**, *85*, 111046. [[CrossRef](#)]
24. Ghamari, M.; Sundaram, S. Solar Wall Technology and Its Impact on Building Performance. *Energies* **2024**, *17*, 1075. [[CrossRef](#)]
25. Tyagi, V.V.; Chopra, K.; Kalidasan, B.; Chauhan, A.; Stritih, U.; Anand, S.; Pandey, A.K.; Sari, A.; Kothari, R. Phase Change Material Based Advance Solar Thermal Energy Storage Systems for Building Heating and Cooling Applications: A Prospective Research Approach. *Sustain. Energy Technol. Assess.* **2021**, *47*, 101318. [[CrossRef](#)]
26. Ghamari, M.; See, C.H.; Hughes, D.; Mallick, T.; Reddy, K.S.; Patchigolla, K.; Sundaram, S. Advancing Sustainable Building through Passive Cooling with Phase Change Materials, a Comprehensive Literature Review. *Energy Build.* **2024**, *312*, 114164. [[CrossRef](#)]

27. Chowdhary, N.; Barbui, C.; Anstey, K.J.; Kivipelto, M.; Barbera, M.; Peters, R.; Zheng, L.; Kulmala, J.; Stephen, R.; Ferri, C.P.; et al. Reducing the Risk of Cognitive Decline and Dementia: WHO Recommendations. *Front. Neurol.* **2022**, *12*, 765584. [[CrossRef](#)] [[PubMed](#)]
28. Şirin, C.; Goggins, J.; Hajdukiewicz, M. A Review on Building-Integrated Photovoltaic/Thermal Systems for Green Buildings. *Appl. Therm. Eng.* **2023**, *229*, 120607. [[CrossRef](#)]
29. Gupta, V.; Deb, C. Envelope Design for Low-Energy Buildings in the Tropics: A Review. *Renew. Sustain. Energy Rev.* **2023**, *186*, 113650. [[CrossRef](#)]
30. Durakovic, B.; Halilovic, M. Thermal Performance Analysis of PCM Solar Wall under Variable Natural Conditions: An Experimental Study. *Energy Sustain. Dev.* **2023**, *76*, 101274. [[CrossRef](#)]
31. Umoh, A.A.; Adefemi, A.; Ibewe, K.I.; Etukudoh, E.A.; Ilojiyanya, V.I.; Nwokediegwu, Z.Q.S. Green architecture and energy efficiency: A review of innovative design and construction techniques. *Eng. Sci. Technol. J.* **2024**, *5*, 185–200. [[CrossRef](#)]
32. Piselli, C.; Prabhakar, M.; de Gracia, A.; Saffari, M.; Pisello, A.L.; Cabeza, L.F. Optimal Control of Natural Ventilation as Passive Cooling Strategy for Improving the Energy Performance of Building Envelope with PCM Integration. *Renew. Energy* **2020**, *162*, 171–181. [[CrossRef](#)]
33. Yaman, M. Different Façade Types and Building Integration in Energy Efficient Building Design Strategies. *Int. J. Built Environ. Sustain.* **2021**, *8*, 49–61. [[CrossRef](#)]
34. Faramarzi, A.; Stephens, B.; Heidarinejad, M. Optimal Control of Switchable Ethylene-Tetrafluoroethylene (ETFE) Cushions for Building Façades. *Sol. Energy* **2021**, *218*, 180–194. [[CrossRef](#)]
35. Bougiatioti, F.; Alexandrou, E.; Katsaros, M. Sustainable Refurbishment of Existing, Typical Single-Family Residential Buildings in Greece. *Int. J. Build. Pathol. Adapt.* **2023**. online ahead of print. [[CrossRef](#)]
36. Al Dakheel, J.; Tabet Aoul, K. Building Applications, Opportunities and Challenges of Active Shading Systems: A State-of-the-Art Review. *Energies* **2017**, *10*, 1672. [[CrossRef](#)]
37. Guo, W.; Kong, L.; Chow, T.; Li, C.; Zhu, Q.; Qiu, Z.; Li, L.; Wang, Y.; Riffat, S.B. Energy Performance of Photovoltaic (PV) Windows under Typical Climates of China in Terms of Transmittance and Orientation. *Energy* **2020**, *213*, 118794. [[CrossRef](#)]
38. Tushar, Q.; Bhuiyan, M.A.; Zhang, G. Energy Simulation and Modeling for Window System: A Comparative Study of Life Cycle Assessment and Life Cycle Costing. *J. Clean. Prod.* **2022**, *330*, 129936. [[CrossRef](#)]
39. Schünemann, C.; Schiela, D.; Ortlepp, R. How Window Ventilation Behaviour Affects the Heat Resilience in Multi-Residential Buildings. *Build. Environ.* **2021**, *202*, 107987. [[CrossRef](#)]
40. Lee, J.W.; Jung, H.J.; Park, J.Y.; Lee, J.B.; Yoon, Y. Optimization of Building Window System in Asian Regions by Analyzing Solar Heat Gain and Daylighting Elements. *Renew. Energy* **2013**, *50*, 522–531. [[CrossRef](#)]
41. Sun, Y.; Liu, D.; Flor, J.-F.; Shank, K.; Baig, H.; Wilson, R.; Liu, H.; Sundaram, S.; Mallick, T.K.; Wu, Y. Analysis of the Daylight Performance of Window Integrated Photovoltaics Systems. *Renew. Energy* **2020**, *145*, 153–163. [[CrossRef](#)]
42. Ahmed, M.M.S.; Radwan, A.; Serageldin, A.A.; Abdeen, A.; Abo-Zahhad, E.M.; Nagano, K. The Thermal Potential of a New Multifunctional Sliding Window. *Sol. Energy* **2021**, *226*, 389–407. [[CrossRef](#)]
43. Evola, G.; Gullo, F.; Marletta, L. The Role of Shading Devices to Improve Thermal and Visual Comfort in Existing Glazed Buildings. *Energy Procedia* **2017**, *134*, 346–355. [[CrossRef](#)]
44. Zheng, X.; Huang, A.; Xiao, Y.; Qu, D.; Qin, G. A fiber-based sandwich evaporator for effective solar evaporation and salt-rejection performance. *Desalination* **2024**, *577*, 117416. [[CrossRef](#)]
45. Yao, J.; Zhu, N. Evaluation of Indoor Thermal Environmental, Energy and Daylighting Performance of Thermotropic Windows. *Build. Environ.* **2012**, *49*, 283–290. [[CrossRef](#)]
46. Zhao, J.; Du, Y. Multi-Objective Optimization Design for Windows and Shading Configuration Considering Energy Consumption and Thermal Comfort: A Case Study for Office Building in Different Climatic Regions of China. *Sol. Energy* **2020**, *206*, 997–1017. [[CrossRef](#)]
47. Rizwan, M.; Khan, W.S.; Zaman, K. Polycrystalline silicon solar cells. In *Green Sustainable Process for Chemical and Environmental Engineering and Science*; Elsevier: Amsterdam, The Netherlands, 2021; pp. 271–285. [[CrossRef](#)]
48. Debbarma, M.; Sudhakar, K.; Baredar, P. Thermal Modeling, Exergy Analysis, Performance of BIPV and BIPVT: A Review. *Renew. Sustain. Energy Rev.* **2017**, *73*, 1276–1288. [[CrossRef](#)]
49. Weller, B.; Hemmerle, C.; Jakubetz, S.; Unnewehr, S. *Detail Practice: Photovoltaics*; DETAIL—Institut für Internationale Architektur-Dokumentation GmbH & Co. KG: Munich, Germany, 2010; ISBN 978-3-0346-0369-0.
50. Karthick, A.; Kalidasa Murugavel, K.; Kalaivani, L.; Saravana Babu, U. Performance Study of Building Integrated Photovoltaic Modules. *Adv. Build. Energy Res.* **2018**, *12*, 178–194. [[CrossRef](#)]
51. Peng, J.; Lu, L.; Yang, H. An Experimental Study of the Thermal Performance of a Novel Photovoltaic Double-Skin Façade in Hong Kong. *Sol. Energy* **2013**, *97*, 293–304. [[CrossRef](#)]
52. Peng, J.; Curcija, D.C.; Lu, L.; Selkowitz, S.E.; Yang, H.; Zhang, W. Numerical Investigation of the Energy Saving Potential of a Semi-Transparent Photovoltaic Double-Skin Façade in a Cool-Summer Mediterranean Climate. *Appl. Energy* **2016**, *165*, 345–356. [[CrossRef](#)]
53. Luo, Y.; Zhang, L.; Liu, Z.; Xie, L.; Wang, X.; Wu, J. Experimental Study and Performance Evaluation of a PV-Blind Embedded Double Skin Façade in Winter Season. *Energy* **2018**, *165*, 326–342. [[CrossRef](#)]

54. Wang, M.; Peng, J.; Li, N.; Yang, H.; Wang, C.; Li, X.; Lu, T. Comparison of Energy Performance between PV Double Skin Facades and PV Insulating Glass Units. *Appl. Energy* **2017**, *194*, 148–160. [[CrossRef](#)]
55. Preet, S.; Sharma, M.K.; Mathur, J.; Chowdhury, A.; Mathur, S. Performance Evaluation of Photovoltaic Double-Skin Facade with Forced Ventilation in the Composite Climate. *J. Build. Eng.* **2020**, *32*, 101733. [[CrossRef](#)]
56. Zomer, C.; Custódio, I.; Antonioli, A.; Rütther, R. Performance Assessment of Partially Shaded Building-Integrated Photovoltaic (BIPV) Systems in a Positive-Energy Solar Energy Laboratory Building: Architecture Perspectives. *Sol. Energy* **2020**, *211*, 879–896. [[CrossRef](#)]
57. Stoichkov, V.; Sweet, T.K.N.; Jenkins, N.; Kettle, J. Studying the Outdoor Performance of Organic Building-Integrated Photovoltaics Laminated to the Cladding of a Building Prototype. *Sol. Energy Mater. Sol. Cells* **2019**, *191*, 356–364. [[CrossRef](#)]
58. Tak, S.; Woo, S.; Park, J.; Park, S. Effect of the Changeable Organic Semi-Transparent Solar Cell Window on Building Energy Efficiency and User Comfort. *Sustainability* **2017**, *9*, 950. [[CrossRef](#)]
59. Chung, M.H.; Park, B.R.; Choi, E.J.; Choi, Y.J.; Lee, C.; Hong, J.; Cho, H.U.; Cho, J.H.; Moon, J.W. Performance Level Criteria for Semi-Transparent Photovoltaic Windows Based on Dye-Sensitized Solar Cells. *Sol. Energy Mater. Sol. Cells* **2020**, *217*, 110683. [[CrossRef](#)]
60. Wang, D.; Qi, T.; Liu, Y.; Wang, Y.; Fan, J.; Wang, Y.; Du, H. A Method for Evaluating Both Shading and Power Generation Effects of Rooftop Solar PV Panels for Different Climate Zones of China. *Sol. Energy* **2020**, *205*, 432–445. [[CrossRef](#)]
61. Xiao, Y.; Tian, W.; Yu, L.; Chen, M.; Zheng, X.; Qin, G. Tunable optical properties of ATO-CuO hybrid nanofluids and the application as spectral beam splitters. *Energy* **2024**, *289*, 129964. [[CrossRef](#)]
62. Xiao, Y.; Bao, Y.; Yu, L.; Zheng, X.; Qin, G.; Chen, M.; He, M. Ultra-stable carbon quantum dot nanofluids as excellent spectral beam splitters in PV/T applications. *Energy* **2023**, *273*, 127159. [[CrossRef](#)]
63. Mun, S.-H.; Kang, J.; Kwak, Y.; Jeong, Y.-S.; Lee, S.-M.; Huh, J.-H. Limitations of EnergyPlus in Analyzing Energy Performance of Semi-Transparent Photovoltaic Modules. *Case Stud. Therm. Eng.* **2020**, *22*, 100765. [[CrossRef](#)]
64. Roberts, F.; Yang, S.; Du, H.; Yang, R. Effect of semi-transparent a-Si PV glazing within double-skin façades on visual and energy performances under the UK climate condition. *Renew. Energy* **2023**, *207*, 601–610. [[CrossRef](#)]
65. Tinedert, I.E.; Pezzimenti, F.; Megherbi, M.L.; Saadoun, A. Design and Simulation of a High Efficiency CdS/CdTe Solar Cell. *Optik* **2020**, *208*, 164112. [[CrossRef](#)]
66. Doroody, C.; Rahman, K.S.; Kiong, T.S.; Amin, N. Optoelectrical Impact of Alternative Window Layer Composition in CdTe Thin Film Solar Cells Performance. *Sol. Energy* **2022**, *233*, 523–530. [[CrossRef](#)]
67. Anctil, A.; Lee, E.; Lunt, R.R. Net Energy and Cost Benefit of Transparent Organic Solar Cells in Building-Integrated Applications. *Appl. Energy* **2020**, *261*, 114429. [[CrossRef](#)]
68. Liu, C.; Xiao, C.; Xie, C.; Li, W. Flexible Organic Solar Cells: Materials, Large-Area Fabrication Techniques and Potential Applications. *Nano Energy* **2021**, *89*, 106399. [[CrossRef](#)]
69. Kim, J.-H.; Han, S.-H. Energy Generation Performance of Window-Type Dye-Sensitized Solar Cells by Color and Transmittance. *Sustainability* **2020**, *12*, 8961. [[CrossRef](#)]
70. Raoui, Y.; Ez-Zahraouy, H.; Ahmad, S.; Kazim, S. Unravelling the Theoretical Window to Fabricate High Performance Inorganic Perovskite Solar Cells. *Sustain. Energy Fuels* **2021**, *5*, 219–229. [[CrossRef](#)]
71. Chen, C.; Zhou, Z.; Jiang, Y.; Feng, Y.; Fang, Y.; Liu, J.; Chen, M.; Liu, J.; Gao, J.; Feng, S.-P. Additive Engineering in Antisolvent for Widening the Processing Window and Promoting Perovskite Seed Formation in Perovskite Solar Cells. *ACS Appl. Mater. Interfaces* **2022**, *14*, 17348–17357. [[CrossRef](#)] [[PubMed](#)]
72. Xuan, Q.; Li, G.; Lu, Y.; Zhao, B.; Wang, F.; Pei, G. Daylighting Utilization and Uniformity Comparison for a Concentrator-Photovoltaic Window in Energy Saving Application on the Building. *Energy* **2021**, *214*, 118932. [[CrossRef](#)]
73. Li, G.; Xuan, Q.; Akram, M.W.; Golizadeh Akhlaghi, Y.; Liu, H.; Shittu, S. Building Integrated Solar Concentrating Systems: A Review. *Appl. Energy* **2020**, *260*, 114288. [[CrossRef](#)]
74. Liu, X.; Wu, Y. A Review of Advanced Architectural Glazing Technologies for Solar Energy Conversion and Intelligent Daylighting Control. *Archit. Intell.* **2022**, *1*, 10. [[CrossRef](#)]
75. Uematsu, T.; Yazawa, Y.; Tsutsui, K.; Miyamura, Y.; Ohtsuka, H.; Warabisako, T.; Joge, T. Design and Characterization of Flat-Plate Static-Concentrator Photovoltaic Modules. *Sol. Energy Mater. Sol. Cells* **2001**, *67*, 441–448. [[CrossRef](#)]
76. Liu, X.; Wu, Y.; Hou, X.; Liu, H. Investigation of the Optical Performance of a Novel Planar Static PV Concentrator with Lambertian Rear Reflectors. *Buildings* **2017**, *7*, 88. [[CrossRef](#)]
77. Weber, K.J.; Everett, V.; Deenapanray, P.N.K.; Franklin, E.; Blakers, A.W. Modeling of Static Concentrator Modules Incorporating Lambertian or V-Groove Rear Reflectors. *Sol. Energy Mater. Sol. Cells* **2006**, *90*, 1741–1749. [[CrossRef](#)]
78. Wu, Y.; Connelly, K.; Liu, Y.; Gu, X.; Gao, Y.; Chen, G.Z. Smart Solar Concentrators for Building Integrated Photovoltaic Façades. *Sol. Energy* **2016**, *133*, 111–118. [[CrossRef](#)]
79. Kim, J.M.; Dutta, P.S. Optical Efficiency–Concentration Ratio Trade-off for a Flat Panel Photovoltaic System with Diffuser Type Concentrator. *Sol. Energy Mater. Sol. Cells* **2012**, *103*, 35–40. [[CrossRef](#)]
80. Luger, R.; Agol, E.; Bartolić, F.; Foreman-Mackey, D. Analytic Light Curves in Reflected Light: Phase Curves, Occultations, and Non-Lambertian Scattering for Spherical Planets and Moons. *Astron. J.* **2022**, *164*, 4. [[CrossRef](#)]
81. Manzoor, S.; Filipič, M.; Onno, A.; Topič, M.; Holman, Z.C. Visualizing Light Trapping within Textured Silicon Solar Cells. *J. Appl. Phys.* **2020**, *127*, 063104. [[CrossRef](#)]

82. Chemisana, D.; Collados, M.V.; Quintanilla, M.; Atencia, J. Holographic Lenses for Building Integrated Concentrating Photovoltaics. *Appl. Energy* **2013**, *110*, 227–235. [[CrossRef](#)]
83. Zhang, D. One-Axis Tracking Holographic Planar Concentrator Systems. *J. Photonics Energy* **2011**, *1*, 015505. [[CrossRef](#)]
84. Marín-Sáez, J.; Chemisana, D.; Atencia, J.; Collados, M.-V. Outdoor Performance Evaluation of a Holographic Solar Concentrator Optimized for Building Integration. *Appl. Energy* **2019**, *250*, 1073–1084. [[CrossRef](#)]
85. Ludman, J.; Riccobono, J.; Reinhand, N.; Semenova, I.; Martin, J.; Tai, W.; Xiao, L.L.; Syphers, G. Holographic Solar Concentrator for Terrestrial Photovoltaics. In Proceedings of the 1994 IEEE 1st World Conference on Photovoltaic Energy Conversion—WCPEC (A Joint Conference of PVSC, PVSEC and PSEC), Waikoloa, HI, USA, 5–9 December 1994; pp. 1208–1215.
86. Stojanoff, C.G. Engineering Applications of HOEs Manufactured with Enhanced Performance DCG Films. In *Practical Holography XX: Materials and Applications*; Bjelkhagen, H.I., Lessard, R.A., Eds.; SPIE: Cergy-Pontoise, France, 2006; p. 613601.
87. Ferrara, M.A.; Borbone, F.; Coppola, G. Holographic Optical Lenses Recorded on a Glassy Matrix-Based Photopolymer for Solar Concentrators. *Photonics* **2021**, *8*, 585. [[CrossRef](#)]
88. Kalinina, A.A.; Putilin, A.N.; Kopenkin, S.S. Axial Holographic Optical Elements Implementation in Augmented Reality Systems. *Bull. Lebedev Phys. Inst.* **2023**, *50*, 311–317. [[CrossRef](#)]
89. Vorndran, S.; Russo, J.M.; Wu, Y.; Gordon, M.; Kostuk, R. Holographic Diffraction-through-Aperture Spectrum Splitting for Increased Hybrid Solar Energy Conversion Efficiency. *Int. J. Energy Res.* **2015**, *39*, 326–335. [[CrossRef](#)]
90. Zhao, J.; Chrysler, B.; Kostuk, R.K. Holographic Low Concentration Optical System Increasing Light Collection Efficiency of Regular Solar Panels. *J. Photonics Energy* **2021**, *11*, 027002. [[CrossRef](#)]
91. Lin, J.; Wang, L.; Jing, Q.; Zhao, H. Highly Efficient and High Color Rendering Index Multilayer Luminescent Solar Concentrators Based on Colloidal Carbon Quantum Dots. *Chem. Eng. J.* **2024**, *481*, 148441. [[CrossRef](#)]
92. Richards, B.S.; Howard, I.A. Luminescent Solar Concentrators for Building Integrated Photovoltaics: Opportunities and Challenges. *Energy Environ. Sci.* **2023**, *16*, 3214–3239. [[CrossRef](#)]
93. Debije, M.G.; Evans, R.C.; Griffini, G. Laboratory Protocols for Measuring and Reporting the Performance of Luminescent Solar Concentrators. *Energy Environ. Sci.* **2021**, *14*, 293–301. [[CrossRef](#)]
94. Mattiello, S.; Sanzone, A.; Bruni, F.; Gandini, M.; Pinchetti, V.; Monguzzi, A.; Facchinetti, I.; Ruffo, R.; Meinardi, F.; Mattioli, G.; et al. Chemically Sustainable Large Stokes Shift Derivatives for High-Performance Large-Area Transparent Luminescent Solar Concentrators. *Joule* **2020**, *4*, 1988–2003. [[CrossRef](#)]
95. Ter Schiphorst, J.; Cheng, M.L.M.K.H.Y.K.; van der Heijden, M.; Hageman, R.L.; Bugg, E.L.; Wagenaar, T.J.L.; Debije, M.G. Printed Luminescent Solar Concentrators: Artistic Renewable Energy. *Energy Build.* **2020**, *207*, 109625. [[CrossRef](#)]
96. Smestad, G.; Ries, H.; Winston, R.; Yablonoitch, E. The Thermodynamic Limits of Light Concentrators. *Sol. Energy Mater.* **1990**, *21*, 99–111. [[CrossRef](#)]
97. Yablonoitch, E. Thermodynamics of the Fluorescent Planar Concentrator. *J. Opt. Soc. Am.* **1980**, *70*, 1362. [[CrossRef](#)]
98. Huld, T.; Müller, R.; Gambardella, A. A New Solar Radiation Database for Estimating PV Performance in Europe and Africa. *Sol. Energy* **2012**, *86*, 1803–1815. [[CrossRef](#)]
99. Friedman, P.S. Luminescent Solar Concentrators. *Opt. Eng.* **1981**, *20*, 206887. [[CrossRef](#)]
100. Alonso-Alvarez, D.; Klampaftis, E.; Ross, D.; Richards, B.S. External Thermalization of Carriers with Luminescent Down Shifting for Lower Operating Solar Cell Temperature. *IEEE J. Photovolt.* **2014**, *4*, 1532–1537. [[CrossRef](#)]
101. Tawalare, P.K. Optimizing photovoltaic conversion of solar energy. *AIP Adv.* **2021**, *11*, 100701. [[CrossRef](#)]
102. Slooff, L.H.; Bende, E.E.; Burgers, A.R.; Budel, T.; Pravettoni, M.; Kenny, R.P.; Dunlop, E.D.; Büchtemann, A. A Luminescent Solar Concentrator with 7.1% Power Conversion Efficiency. *Phys. Status Solidi RRL—Rapid Res. Lett.* **2008**, *2*, 257–259. [[CrossRef](#)]
103. Wilson, L.R.; Klampaftis, E.; Richards, B.S. Enhancement of Power Output from a Large-Area Luminescent Solar Concentrator with 4.8× Concentration via Solar Cell Current Matching. *IEEE J. Photovolt.* **2017**, *7*, 802–809. [[CrossRef](#)]
104. Aste, N.; Tagliabue, L.C.; Del Pero, C.; Testa, D.; Fusco, R. Performance Analysis of a Large-Area Luminescent Solar Concentrator Module. *Renew. Energy* **2015**, *76*, 330–337. [[CrossRef](#)]
105. Zhang, J.; Wang, M.; Zhang, Y.; He, H.; Xie, W.; Yang, M.; Ding, J.; Bao, J.; Sun, S.; Gao, C. Optimization of Large-Size Glass Laminated Luminescent Solar Concentrators. *Sol. Energy* **2015**, *117*, 260–267. [[CrossRef](#)]
106. Anand, A.; Zaffalon, M.L.; Gariano, G.; Camellini, A.; Gandini, M.; Brescia, R.; Capitani, C.; Bruni, F.; Pinchetti, V.; Zavelani-Rossi, M.; et al. Evidence for the Band-Edge Exciton of CuInS₂ Nanocrystals Enables Record Efficient Large-Area Luminescent Solar Concentrators. *Adv. Funct. Mater.* **2020**, *30*, 1906629. [[CrossRef](#)]
107. Baig, H.; Sarmah, N.; Heasman, K.C.; Mallick, T.K. Numerical Modelling and Experimental Validation of a Low Concentrating Photovoltaic System. *Sol. Energy Mater. Sol. Cells* **2013**, *113*, 201–219. [[CrossRef](#)]
108. Shanks, K.; Knowles, A.; Brierley, A.; Baig, H.; Orr, H.; Sun, Y.; Wu, Y.; Sundaram, S.; Mallick, T. An Experimental Analysis of the Optical, Thermal and Power to Weight Performance of Plastic and Glass Optics with AR Coatings for Embedded CPV Windows. *Sol. Energy Mater. Sol. Cells* **2019**, *200*, 110027. [[CrossRef](#)]
109. Baig, H.; Sellami, N.; Chemisana, D.; Rosell, J.; Mallick, T.K. Performance Analysis of a Dielectric Based 3D Building Integrated Concentrating Photovoltaic System. *Sol. Energy* **2014**, *103*, 525–540. [[CrossRef](#)]
110. Baig, H.; Sellami, N.; Mallick, T.K. Trapping Light Escaping from the Edges of the Optical Element in a Concentrating Photovoltaic System. *Energy Convers. Manag.* **2015**, *90*, 238–246. [[CrossRef](#)]

111. Zhu, X.; Debije, M.G.; Reinders, A.H.M.E. The Feasibility of Luminescent Solar Concentrators Overlays for Conventional Lens. In Proceedings of the 2023 IEEE 50th Photovoltaic Specialists Conference (PVSC), San Juan, Puerto Rico, 11–16 June 2023; pp. 1–3.
112. Dudley, V.; Workhoven, R. *Performance Testing of the McDonnell Douglas Fresnel Lens Solar Collector*; EG&G Inc.: Albuquerque, NM, USA; Sandia National Lab.: Albuquerque, NM, USA, 1979.
113. Chemisana, D. Building Integrated Concentrating Photovoltaics: A Review. *Renew. Sustain. Energy Rev.* **2011**, *15*, 603–611. [[CrossRef](#)]
114. Zhu, L.; Shao, Z.; Sun, Y.; Soebarto, V.; Gao, F.; Zillante, G.; Zuo, J. Indoor Daylight Distribution in a Room with Integrated Dynamic Solar Concentrating Facade. *Energy Build.* **2018**, *158*, 1–13. [[CrossRef](#)]
115. Tsoutsou, S.; Infante Ferreira, C.; Krieg, J.; Ezzahiri, M. Building Integration of Concentrating Solar Systems for Heating Applications. *Appl. Therm. Eng.* **2014**, *70*, 647–654. [[CrossRef](#)]
116. Mandalaki, M.; Tsoutsos, T.; Papamanolis, N. Integrated PV in Shading Systems for Mediterranean Countries: Balance between Energy Production and Visual Comfort. *Energy Build.* **2014**, *77*, 445–456. [[CrossRef](#)]
117. Tourasse, G.; Dumortier, D. Development of a System Measuring the Solar Radiation Spectrum in 5 Planes for Daylight and PV Applications. *Energy Procedia* **2014**, *57*, 1110–1119. [[CrossRef](#)]
118. Sabry, M. Prismatic TIR (Total Internal Reflection) Low-Concentration PV (Photovoltaics)-Integrated Façade for Low Latitudes. *Energy* **2016**, *107*, 473–481. [[CrossRef](#)]
119. Mills, D.R.; Giutronich, J.E. Ideal Prism Solar Concentrators. *Sol. Energy* **1978**, *21*, 423–430. [[CrossRef](#)]
120. Winston, R.; Miñano, J.C.; Benítez, P. Nonimaging optical systems. In *Nonimaging Optics*; Elsevier: Amsterdam, The Netherlands, 2005; pp. 43–68.
121. Maruyama, T.; Osako, S. Wedge-Shaped Light Concentrator Using Total Internal Reflection. *Sol. Energy Mater. Sol. Cells* **1999**, *57*, 75–83. [[CrossRef](#)]
122. Uematsu, T.; Yazawa, Y.; Miyamura, Y.; Muramatsu, S.; Ohtsuka, H.; Tsutsui, K.; Warabisako, T. Static Concentrator Photovoltaic Module with Prism Array. *Sol. Energy Mater. Sol. Cells* **2001**, *67*, 415–423. [[CrossRef](#)]
123. Yamada, N.; Kanno, K.; Hayashi, K.; Tokimitsu, T. Performance of See-through Prism CPV Module for Window Integrated Photovoltaics. *Opt. Express* **2011**, *19*, A649. [[CrossRef](#)] [[PubMed](#)]
124. Baig, H.; Sarmah, N.; Chemisana, D.; Rosell, J.; Mallick, T.K. Enhancing Performance of a Linear Dielectric Based Concentrating Photovoltaic System Using a Reflective Film along the Edge. *Energy* **2014**, *73*, 177–191. [[CrossRef](#)]
125. Yu, X.; Su, Y.; Zheng, H.; Riffat, S. A Study on Use of Miniature Dielectric Compound Parabolic Concentrator (DCPC) for Daylighting Control Application. *Build. Env.* **2014**, *74*, 75–85. [[CrossRef](#)]
126. Masood, F.; Nor, N.B.M.; Elamvazuthi, I.; Saidur, R.; Alam, M.A.; Akhter, J.; Yusuf, M.; Ali, S.M.; Sattar, M.; Baba, M. The Compound Parabolic Concentrators for Solar Photovoltaic Applications: Opportunities and Challenges. *Energy Rep.* **2022**, *8*, 13558–13584. [[CrossRef](#)]
127. Gudekar, A.S.; Jadhav, A.S.; Panse, S.V.; Joshi, J.B.; Pandit, A.B. Cost Effective Design of Compound Parabolic Collector for Steam Generation. *Sol. Energy* **2013**, *90*, 43–50. [[CrossRef](#)]
128. Ramirez-Iniguez, R.; Deciga-Gusi, J.; Freier, D.; Abu-Bakar, S.H.; Muhammad-Sukki, F. Experimental Evaluation of a Solar Window Incorporating Rotationally Asymmetrical Compound Parabolic Concentrators (RACPC). *Energy Procedia* **2017**, *130*, 102–107. [[CrossRef](#)]
129. Mallick, T.K.; Eames, P.C. Electrical Performance Evaluation of Low-concentrating Non-imaging Photovoltaic Concentrator. *Prog. Photovolt. Res. Appl.* **2008**, *16*, 389–398. [[CrossRef](#)]
130. Zacharopoulos, A.; Eames, P.C.; McLarnon, D.; Norton, B. Linear Dielectric Non-Imaging Concentrating Covers for PV Integrated Building Facades. *Sol. Energy* **2000**, *68*, 439–452. [[CrossRef](#)]
131. Su, Y.; Pei, G.; Riffat, S.B.; Huang, H. A Novel Lens-Walled Compound Parabolic Concentrator for Photovoltaic Applications. *J. Sol. Energy Eng.* **2012**, *134*, 021010. [[CrossRef](#)]
132. Sharaf, O.Z.; Orhan, M.F. Concentrated Photovoltaic Thermal (CPVT) Solar Collector Systems: Part I—Fundamentals, Design Considerations and Current Technologies. *Renew. Sustain. Energy Rev.* **2015**, *50*, 1500–1565. [[CrossRef](#)]
133. Sarmah, N.; Richards, B.S.; Mallick, T.K. Design, Development and Indoor Performance Analysis of a Low Concentrating Dielectric Photovoltaic Module. *Sol. Energy* **2014**, *103*, 390–401. [[CrossRef](#)]
134. Sarmah, N.; Mallick, T.K. Design, Fabrication and Outdoor Performance Analysis of a Low Concentrating Photovoltaic System. *Sol. Energy* **2015**, *112*, 361–372. [[CrossRef](#)]
135. Mallick, T.; Eames, P. Design and Fabrication of Low Concentrating Second Generation PRIDE Concentrator. *Sol. Energy Mater. Sol. Cells* **2007**, *91*, 597–608. [[CrossRef](#)]
136. Meng, X.; Sellami, N.; Knox, A.R.; Montecucco, A.; Siviter, J.; Mullen, P.; Ashraf, A.; Samarelli, A.; Llin, L.F.; Paul, D.J.; et al. A Novel Absorptive/Reflective Solar Concentrator for Heat and Electricity Generation: An Optical and Thermal Analysis. *Energy Convers. Manag.* **2016**, *114*, 142–153. [[CrossRef](#)]
137. Xuan, Q.; Li, G.; Yang, H.; Gao, C.; Jiang, B.; Liu, X.; Ji, J.; Zhao, X.; Pei, G. Performance Evaluation for the Dielectric Asymmetric Compound Parabolic Concentrator with Almost Unity Angular Acceptance Efficiency. *Energy* **2021**, *233*, 121065. [[CrossRef](#)]
138. Sharma, S.; Tahir, A.; Reddy, K.S.; Mallick, T.K. Performance Enhancement of a Building-Integrated Concentrating Photovoltaic System Using Phase Change Material. *Sol. Energy Mater. Sol. Cells* **2016**, *149*, 29–39. [[CrossRef](#)]

139. Allen, K.; Connelly, K.; Rutherford, P.; Wu, Y. Smart Windows—Dynamic Control of Building Energy Performance. *Energy Build.* **2017**, *139*, 535–546. [[CrossRef](#)]
140. Resch, K.; Wallner, G.M. Thermotropic Layers for Flat-Plate Collectors—A Review of Various Concepts for Overheating Protection with Polymeric Materials. *Sol. Energy Mater. Sol. Cells* **2009**, *93*, 119–128. [[CrossRef](#)]
141. Wang, M.; Gao, Y.; Cao, C.; Chen, K.; Wen, Y.; Fang, D.; Li, L.; Guo, X. Binary Solvent Colloids of Thermosensitive Poly(*N*-Isopropylacrylamide) Microgel for Smart Windows. *Ind. Eng. Chem. Res.* **2014**, *53*, 18462–18472. [[CrossRef](#)]
142. Connelly, K.; Wu, Y.; Chen, J.; Lei, Y. Design and Development of a Reflective Membrane for a Novel Building Integrated Concentrating Photovoltaic (BICPV) ‘Smart Window’ System. *Appl. Energy* **2016**, *182*, 331–339. [[CrossRef](#)]
143. Zhou, Y.; Cai, Y.; Hu, X.; Long, Y. Temperature-Responsive Hydrogel with Ultra-Large Solar Modulation and High Luminous Transmission for “Smart Window” Applications. *J. Mater. Chem. A* **2014**, *2*, 13550–13555. [[CrossRef](#)]
144. Li, X.-H.; Liu, C.; Feng, S.-P.; Fang, N.X. Broadband Light Management with Thermochromic Hydrogel Microparticles for Smart Windows. *Joule* **2019**, *3*, 290–302. [[CrossRef](#)]
145. Mizuntani, M.; Satoh, K.; Kamigaito, M. Degradable Poly(*N*-Isopropylacrylamide) with Tunable Thermosensitivity by Simultaneous Chain- and Step-Growth Radical Polymerization. *Macromolecules* **2011**, *44*, 2382–2386. [[CrossRef](#)]
146. Xia, X.; Tang, S.; Lu, X.; Hu, Z. Formation and Volume Phase Transition of Hydroxypropyl Cellulose Microgels in Salt Solution. *Macromolecules* **2003**, *36*, 3695–3698. [[CrossRef](#)]
147. Zhou, Y.; Wang, S.; Peng, J.; Tan, Y.; Li, C.; Boey, F.Y.C.; Long, Y. Liquid Thermo-Responsive Smart Window Derived from Hydrogel. *Joule* **2020**, *4*, 2458–2474. [[CrossRef](#)]
148. Sun, Y.; Liu, X.; Ming, Y.; Liu, X.; Mahon, D.; Wilson, R.; Liu, H.; Eames, P.; Wu, Y. Energy and Daylight Performance of a Smart Window: Window Integrated with Thermotropic Parallel Slat-Transparent Insulation Material. *Appl. Energy* **2021**, *293*, 116826. [[CrossRef](#)]
149. Sun, Y.; Wilson, R.; Liu, H.; Wu, Y. Numerical Investigation of a Smart Window System with Thermotropic Parallel Slat Transparent Insulation Material for Building Energy Conservation and Daylight Autonomy. *Build. Env.* **2021**, *203*, 108048. [[CrossRef](#)]
150. Favoino, F.; Fiorito, F.; Cannavale, A.; Ranzi, G.; Overend, M. Optimal Control and Performance of Photovoltachromic Switchable Glazing for Building Integration in Temperate Climates. *Appl. Energy* **2016**, *178*, 943–961. [[CrossRef](#)]
151. Ma, R.-H.; Chen, Y.-C. BIPV-Powered Smart Windows Utilizing Photovoltaic and Electrochromic Devices. *Sensors* **2011**, *12*, 359–372. [[CrossRef](#)] [[PubMed](#)]
152. MARCHWIŃSKI, J. Theoretical Models of PV-EC Windows Based on the Architectural Analysis of PV-EC Technologies. *Archit. Civ. Eng. Environ.* **2022**, *15*, 95–107. [[CrossRef](#)]
153. Wheeler, L.M.; Moore, D.T.; Ihly, R.; Stanton, N.J.; Miller, E.M.; Tenent, R.C.; Blackburn, J.L.; Neale, N.R. Switchable Photovoltaic Windows Enabled by Reversible Photothermal Complex Dissociation from Methylammonium Lead Iodide. *Nat. Commun.* **2017**, *8*, 1722. [[CrossRef](#)] [[PubMed](#)]
154. Murray, J.; Ma, D.; Munday, J.N. Electrically Controllable Light Trapping for Self-Powered Switchable Solar Windows. *ACS Photonics* **2017**, *4*, 1–7. [[CrossRef](#)]
155. Zhou, J.; Gao, Y.; Zhang, Z.; Luo, H.; Cao, C.; Chen, Z.; Dai, L.; Liu, X. VO₂ Thermochromic Smart Window for Energy Savings and Generation. *Sci. Rep.* **2013**, *3*, 3029. [[CrossRef](#)] [[PubMed](#)]
156. Liu, X.; Wu, Y. Numerical Evaluation of an Optically Switchable Photovoltaic Glazing System for Passive Daylighting Control and Energy-Efficient Building Design. *Build. Env.* **2022**, *219*, 109170. [[CrossRef](#)]
157. Liu, X.; Wu, Y. Monte-Carlo Optical Model Coupled with Inverse Adding-Doubling for Building Integrated Photovoltaic Smart Window Design and Characterisation. *Sol. Energy Mater. Sol. Cells* **2021**, *223*, 110972. [[CrossRef](#)]
158. Liu, X.; Wu, Y. Experimental Characterisation of a Smart Glazing with Tuneable Transparency, Light Scattering Ability and Electricity Generation Function. *Appl. Energy* **2021**, *303*, 117521. [[CrossRef](#)]
159. Liu, X.; Wu, Y. Design, Development and Characterisation of a Building Integrated Concentrating Photovoltaic (BICPV) Smart Window System. *Sol. Energy* **2021**, *220*, 722–734. [[CrossRef](#)]
160. Muñoz-Viveros, C.; Pérez-Fargallo, A.; Rubio-Bellido, C. Influence of the Type of Solar Protection on Thermal and Light Performance in Classrooms. *SSRN Electron. J.* **2022**, *8*, 5329–5340. [[CrossRef](#)]
161. Kaasalainen, T.; Mäkinen, A.; Lehtinen, T.; Moisio, M.; Vinha, J. Architectural window design and energy efficiency: Impacts on heating, cooling and lighting needs in Finnish climates. *J. Build. Eng.* **2020**, *27*, 100996. [[CrossRef](#)]
162. Ghisi, E.; Tinker, J.A. An Ideal Window Area concept for energy efficient integration of daylight and artificial light in buildings. *Build. Environ.* **2005**, *40*, 51–61. [[CrossRef](#)]
163. Vossen, F.M.; Aarts, M.P.J.; Debije, M.G. Visual performance of red luminescent solar concentrating windows in an office environment. *Energy Build.* **2016**, *113*, 123–132. [[CrossRef](#)]
164. Elghamry, R.; Hassan, H. Impact of window parameters on the building envelope on the thermal comfort, energy consumption and cost and environment. *Int. J. Vent.* **2019**, *19*, 233–259. [[CrossRef](#)]

Disclaimer/Publisher’s Note: The statements, opinions and data contained in all publications are solely those of the individual author(s) and contributor(s) and not of MDPI and/or the editor(s). MDPI and/or the editor(s) disclaim responsibility for any injury to people or property resulting from any ideas, methods, instructions or products referred to in the content.